



HAL
open science

Liquid chromatographic isolation of individual carbohydrates from environmental matrices for stable carbon analysis and radiocarbon dating

Amel Nouara, Christos Panagiotopoulos, Jérôme Balesdent, Kalliopi Violaki, Edouard Bard, Yoann Fagault, Daniel James Repeta, Richard Sempere

► To cite this version:

Amel Nouara, Christos Panagiotopoulos, Jérôme Balesdent, Kalliopi Violaki, Edouard Bard, et al.. Liquid chromatographic isolation of individual carbohydrates from environmental matrices for stable carbon analysis and radiocarbon dating. *Analytica Chimica Acta*, 2019, 1067, pp.137-146. 10.1016/j.aca.2019.03.028 . hal-02130025

HAL Id: hal-02130025

<https://hal.science/hal-02130025>

Submitted on 15 May 2019

HAL is a multi-disciplinary open access archive for the deposit and dissemination of scientific research documents, whether they are published or not. The documents may come from teaching and research institutions in France or abroad, or from public or private research centers.

L'archive ouverte pluridisciplinaire **HAL**, est destinée au dépôt et à la diffusion de documents scientifiques de niveau recherche, publiés ou non, émanant des établissements d'enseignement et de recherche français ou étrangers, des laboratoires publics ou privés.

1 **Liquid chromatographic isolation of individual carbohydrates from**
2 **environmental matrices for stable carbon analysis and radiocarbon**
3 **dating**

4
5 **Amel Nouara¹, Christos Panagiotopoulos^{1*}, Jérôme Balesdent², Kalliopi Violaki¹,**
6 **Edouard Bard², Yoann Fagault², Daniel James Repeta³, Richard Sempéré¹**

7
8
9 ¹Aix Marseille Univ., Université de Toulon, CNRS, IRD, MIO UM 110, 13288,
10 Marseille, France

11
12 ²Aix Marseille Univ., CNRS, Collège de France, IRD, INRA, CEREGE UM34, 13545
13 Aix-en-Provence, France

14
15 ³Department of Marine Chemistry and Geochemistry, Woods Hole Oceanographic
16 Institution, Woods Hole, MA 02543, USA

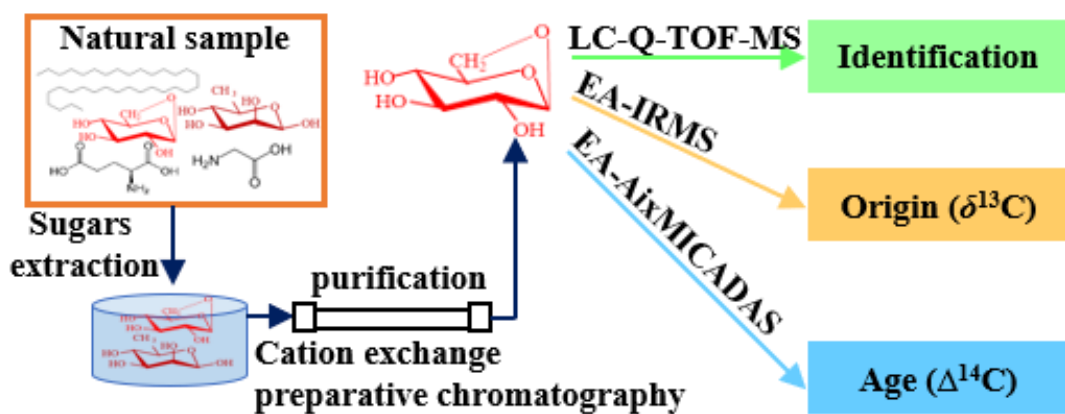
17
18 *Corresponding author. Phone: +33 4 86 09 05 26

19 E-mail : christos.panagiotopoulos@mio.osupytheas.fr

20 Revised version

21 February 27, 2019

22



23

24 Abstract

25 Carbohydrates are among the most abundant organic molecules in both aquatic and
 26 terrestrial ecosystems; however, very few studies have addressed their isotopic signature
 27 using compound-specific isotope analysis, which provides additional information on
 28 their origin ($\delta^{13}\text{C}$) and fate ($\Delta^{14}\text{C}$). In this study, semi-preparative liquid
 29 chromatography with refractive index detection (HPLC-RI) was employed to produce
 30 pure carbohydrate targets for subsequent offline $\delta^{13}\text{C}$ and $\Delta^{14}\text{C}$ isotopic analysis. $\delta^{13}\text{C}$
 31 analysis was performed by elemental analyzer-isotope ratio mass spectrometer
 32 (EA-IRMS) whereas $\Delta^{14}\text{C}$ analysis was performed by an innovative measurement
 33 procedure based on the direct combustion of the isolated fractions using an elemental
 34 analyzer coupled to the gas source of a mini carbon dating system (AixMICADAS). In
 35 general, four successive purifications with Na^+ , Ca^{2+} , Pb^{2+} , and Ca^{2+} cation-exchange
 36 columns were sufficient to produce pure carbohydrates. These carbohydrates were
 37 subsequently identified using mass spectrometry by comparing their mass spectra with
 38 those of authentic standards.

39 The applicability of the proposed method was tested on two different environmental
 40 samples comprising marine particulate organic matter (POM) and total suspended
 41 atmospheric particles (TSP). The obtained results revealed that for the marine POM

42 sample, the $\delta^{13}\text{C}$ values of the individual carbohydrates ranged from -18.5 to -16.8% ,
43 except for levoglucosan and mannosan, which presented values of -27.2 and -26.2% ,
44 respectively. For the TSP sample, the $\delta^{13}\text{C}$ values ranged from -26.4 to -25.0% . The
45 galactose and glucose $\Delta^{14}\text{C}$ values were 19 and 43% , respectively, for the POM sample.
46 On the other hand, the levoglucosan radiocarbon value was 33% for the TSP sample.
47 These results suggest that these carbohydrates exhibit a modern age in both of these
48 samples. Radiocarbon HPLC collection window blanks, measured after the addition of
49 phthalic acid (^{14}C free blank), ranged from -988 to -986% for the abovementioned
50 compounds, indicating a very small background isotopic influence from the whole
51 purification procedure. Overall, the proposed method does not require derivatization
52 steps, produces extremely low blanks, and may be applied to different types of
53 environmental samples.

54

55

56 **Keywords:** Semi-preparative liquid chromatography; carbohydrates purification;
57 carbohydrate-specific ^{13}C and ^{14}C analysis; EA-IRMS; EA-AixMICADAS

58

59 **1. Introduction**

60 Carbohydrates are among the most ubiquitous organic molecules and have been
61 recorded in all geochemical systems, including terrestrial [1,2], marine [3,4], and
62 atmospheric organic matter [5,6]. Although previous investigations have provided a
63 wealth of information on their concentrations and distributions in all geochemical
64 systems [7–11], very less is known about their sources and fate, which have not been
65 thoroughly studied using carbon isotopes. Such information, obtained from carbon

66 isotope examination at the molecular level, may help trace the origin of the different
67 components of organic matter and explain its reactivity during long-range transport
68 [12].

69 Bulk carbon isotope analysis generally reflects the average of the isotopic
70 composition of the whole panel of organic molecules inside the sample [13–18]. Further
71 extraction of the sample with acids or organic solvents produces “purified” fractions
72 (e.g. sugar- or lipid-like fractions) and aids in the determination of the isotopic
73 composition of the hydrophilic and hydrophobic components of the sample [18–20]. For
74 example, previous studies on dissolved organic matter (DOM) have reported $\delta^{13}\text{C}$
75 values for carbohydrate-like fractions in the ranges -29 to -25% in river estuaries [21]
76 and -21.5 to -20.3% in the Atlantic and Pacific Oceans [22]. These $\delta^{13}\text{C}$ values are
77 typical for terrestrial and marine ecosystems, respectively. Moreover, the reported $\Delta^{14}\text{C}$
78 values for carbohydrate-like fractions in marine high molecular weight DOM showed a
79 wide range of values spanning from 7 to -406% , further implying that the age of
80 carbohydrates spans from modern to very old (4180 yr BP) [22]. However, the bulk
81 isotope analysis approach does not completely address the isotopic diversity of the
82 individual molecules inside the sample.

83 In contrast with bulk isotope analysis, the compound-specific isotope analysis
84 (CSIA) of the individual sugars offers valuable information on the origin ($\delta^{13}\text{C}$) and
85 age ($\Delta^{14}\text{C}$) of the single molecules [23–27]. The CSIA technique is not a new approach;
86 however, it requires high analytical skills for the purification and extraction of
87 individual molecules from the sample. This step is crucial and might strongly affect the
88 results. The two most commonly employed techniques for the stable carbon isotope
89 analysis of carbohydrates are gas and liquid chromatography coupled with isotope ratio
90 mass spectrometry (GC-IRMS and LC-IRMS, respectively). Since carbohydrates are

91 not volatile, derivatization steps (silylation or alditol acetate derivatization) are required
92 for GC-IRMS analysis. This further necessitates carbon corrections on the carbohydrate
93 isotopic signatures [23,28–30]. Another disadvantage of the GC-IRMS technique is that
94 two different monosaccharides (e.g. glucose and fructose) can produce the same alditol
95 (e.g. glucitol) during the reduction step of the derivatization procedure, thereby causing
96 a loss of compositional information [31].

97 LC-IRMS is a good alternative to GC-IRMS because it does not require any
98 derivatization steps [30,32–34]. However, this technique does not target all the sugar
99 components of the sample; for example, neutral sugars, amino sugars, alditols, and
100 anhydrosugars cannot be separated in a single run [35,36]. Moreover, both the GC-
101 IRMS and LC-IRMS techniques cannot be used for $\Delta^{14}\text{C}$ determination on single
102 carbohydrates due to their low sensitivity toward the ^{14}C isotope. To date, very few
103 radiocarbon data exist on single carbohydrates comprising neutral sugars, alditols, and
104 anhydrosugars. Alditols and anhydrosugars are important tracers of terrestrial
105 vegetation [37,38] and burning biomass processes [39], respectively. Thus, their
106 isotopic study may help to evaluate their long-range transport from land to sea and more
107 importantly, to assess their reactivity in long time scales (fate) in the marine
108 environment. Although a significant amount of work was done on the compound-
109 specific radiocarbon analysis of individual lipids over the past 20 years [40–43] and
110 more recently, on amino acids [44], a well-established technique for single carbohydrate
111 purification from environmental samples for subsequent radiocarbon measurements has
112 not been reported to date.

113 An interesting approach to produce pure carbohydrate targets for $\delta^{13}\text{C}$ and $\Delta^{14}\text{C}$
114 analysis is the use of semi-preparative high-performance liquid chromatography with
115 refractive index detection (HPLC-RI) on cation-exchange columns. Pure carbohydrates

116 can be analyzed by an elemental analyzer–isotope ratio mass spectrometer (EA-IRMS)
117 for $\delta^{13}\text{C}$ and/or an accelerated mass spectrometer for $\Delta^{14}\text{C}$ analysis. HPLC-RI is a
118 simple and well-established method for carbohydrate analysis; however, in
119 environmental studies, it has been less explored [27,45] than traditional GC-MS or
120 high-performance anion-exchange chromatography with pulsed amperometric detection
121 (HPAEC-PAD) techniques [5,8,10,11,31,46,47].

122 This study employs HPLC-RI to demonstrate that four successive purifications on
123 Na^+ , Ca^{2+} , Pb^{2+} , and Ca^{2+} cation-exchange columns are sufficient to produce pure
124 carbohydrates for compound-specific carbon isotope determination. In previous
125 investigations, the isolated fractions were measured after combustion in evacuated
126 quartz tubes and the produced CO_2 was purified on vacuum lines. This was followed by
127 graphitization for solid measurements or transfer in glass ampoules for gas
128 measurements. On the other hand, this study employs an alternative procedure [48]
129 based on the direct combustion of isolated fractions using an elemental analyzer
130 coupled to the gas source of a mini carbon dating system (AixMICADAS) for $\Delta^{14}\text{C}$
131 analysis. Compared to the time-consuming vacuum line method, this procedure is
132 relatively fast and can be adapted for sample masses $\leq 10 \mu\text{g C}$ with moderate precision.
133 The applicability of the method was tested on two different environmental samples,
134 namely marine particulate organic matter (POM) and total suspended atmospheric
135 particles (TSP).

136 **2. Materials and Methods**

137 *2.1. Chemicals and reagents*

138 All the carbohydrate standards used in this study were purchased from
139 Sigma-Aldrich or Interchim at the purest available grade (>98%). The standard stock

140 solutions of the individual (1 mM) and a mixture of 14 monosaccharides (glucose,
141 galactose, mannose, fucose, rhamnose, arabinose, xylose, fructose, xylitol, sorbitol,
142 mannitol, levoglucosan, mannosan, and galactosan, 1 mM and 50 μ M each) were
143 prepared by dilution with ultrapure water. The prepared solutions were stored in the
144 dark at -15 °C until use. HCl (37%, Sigma-Aldrich), diluted with ultrapure water (final
145 concentration of 1 M), was used for sample hydrolysis. The ultrapure water used in this
146 work was produced by a Millipore Milli-Q system (Molsheim, France).

147 *2.2. Sampling and carbohydrate extraction*

148 *2.2.1. Marine POM*

149 Sinking particles (marine POM) were collected over seven-day periods from January
150 6th to March 3th, 2013, in the upwelling system located offshore Lima (Peru) in the
151 Pacific Ocean ($12^{\circ} 02' S - 77^{\circ} 40' W$), using sediment traps (PPS3, Technicap)
152 deployed in the oxycline/upper oxygen minimum zone (OMZ) layer at a depth of 34 m
153 [49]. To avoid POM bio-degradation, a solution of seawater with 5% formaldehyde was
154 added to the bottom of the collection chamber. After trap recovery, the living and dead
155 swimmers were carefully removed so that only detrital particles remained in the sample.
156 These detrital particles (marine POM) were stored in the dark at 4 °C in the initial
157 chambers used in the PPS3. On land, the samples were filtered through 25 mm
158 pre-combusted (450 °C, 6 h) Whatman GF/F filters (nominal retention size, 0.7 μ m),
159 freeze-dried, and subsequently stored in the dark at 4 °C until further analysis. The
160 organic carbon (OC) content of the particles was in the range 20–29%. To obtain
161 sufficient material for isotopic analysis, five portions (40–60 mg each) of each of the
162 five samples obtained from the respective collection chambers of the sediment trap were
163 pooled together. This resulted in ~ 265 mg dry POM powder which was hydrolyzed with
164 1 M HCl at 100 °C for 20 h [50]. The acid-soluble fraction recovered after

165 centrifugation (2000 rpm) was then transferred into a pre-combusted (450 °C, 6 h) glass
166 vial and the acid was removed from the sample by three successive lyophilizations. The
167 afforded dry powder was weighed (25.61 mg), redissolved in 1 mL ultrapure water and
168 filtered through a Pasteur pipette packed with quartz wool (both pre-combusted at 450
169 °C for 6 h) to remove any remaining particles prior to chromatographic injection.

170 2.2.2. TSP

171 The aerosol sample was collected on a pre-combusted (450 °C, 6 h) weighed
172 Whatman quartz fiber filter (20.3 cm × 25.4 cm) using an automatic sampler (Tisch
173 Environmental USA; flow rate 85 m³ h⁻¹). The sample was collected from the 10th to
174 17th March, 2016, from the rooftop of the Endoume marine station (Marseille; 43° 16'
175 N - 5° 21' E). After collection, the sample was dried for 24 h in a desiccator, weighed,
176 and then stored in a freezer at -25 °C in pre-combusted aluminum foil (450 °C, 6 h).
177 Three portions (17.34 cm² each) of the filter were extracted with 18 mL ultrapure water
178 in an ultrasonic bath for 1 h and then filtered through a Pasteur pipette packed with
179 quartz wool (both pre-combusted at 450 °C for 6 h) to remove any remaining particles
180 [5]. Finally, the sample was freeze-dried and stored in a freezer at -35 °C until
181 chromatographic injection.

182 2.3. Chromatography

183 The carbohydrates were analyzed using an HPLC system (Thermo Scientific
184 UltiMate 3000) equipped with a vacuum degasser and a 100-μL loop auto-injector. The
185 carbohydrates were detected with a refractive index detector (Shodex RI-101) and
186 eluted in isocratic mode with ultrapure water, which was previously degassed with high
187 purity N₂ for 30 min.

188 Three cation-exchange analytical columns packed with a polymeric resin (sulfonated
189 polystyrene-divinyl benzene) were used to purify the carbohydrates (Table S.1). The

190 first column (Na⁺: 4% cross-linked Na⁺; 200 × 10 mm, 12 μm; REZEX™
191 RNO-Oligosaccharide; Phenomenex) was used to separate the oligosaccharides from
192 the monosaccharides after acid hydrolysis. The column temperature was set at 85 °C
193 and the carbohydrates were eluted with ultrapure water at a flow rate of 0.3 mL min⁻¹.
194 The second column (Ca²⁺: 8% cross-linked Ca²⁺; 300 × 7.8 mm, 9 μm; REZEX™
195 RCM-Monosaccharide; Phenomenex) was used to separate the neutral sugars from
196 sugar alcohols and anhydrosugars. The column temperature was maintained at 85 °C
197 throughout the analysis at a flow rate of 0.6 mL min⁻¹. The third column (Pb²⁺: 8%
198 cross-linked resin Pb²⁺; 300 × 7.8 mm, 8 μm; REZEX™ RPM-Monosaccharide;
199 Phenomenex) was used to further separate the monosaccharides at 75 °C and a flow rate
200 of 0.6 mL min⁻¹. The injected samples never exceeded 10 mg/injection and the columns
201 were cleaned at the end of each day by washing overnight with ultrapure water at a flow
202 rate of 0.1 mL min⁻¹. The carbohydrate fractions and/or individual monosaccharides
203 were collected by an automatic Foxy R1 fraction collector (Teledyne ISCO, USA)
204 placed after the RI detector. The system was controlled via Chromeleon
205 chromatography software (ThermoFisher).

206 The detection limit of the HPLC-RI system was ~1 μM at a signal-to-noise ratio
207 (S/N) of three for all the carbohydrates on the three tested columns; this was in
208 agreement with previous results reported in the literature [51]. The precision of the
209 method was evaluated by calculating the relative standard deviation (RSD%) for six
210 replicate HPLC-RI injections of the standard mixture of the 14 carbohydrates at the 5
211 μM level. The RSD was <10% for the peak area and <1% for the retention time for all
212 the columns tested. Additional details on the system optimization are included in the
213 supplementary information (section S1 and Fig. S1).

214 2.4. Isotopic measurements

215 2.4.1. EA-IRMS

216 Prior to EA-IRMS processing, the samples were acidified with HCl (final
217 concentration, 0.01 M) to avoid any errors related to the isotopic signature of inorganic
218 carbon mainly from atmospheric CO₂ absorbed in the sample [52]. The samples were
219 placed in a tin capsule (5 mm × 9 mm; light; Santis) and dried under a N₂ stream. The
220 stable carbon isotope composition and the carbon content of the purified carbohydrates
221 were measured using an elemental analyzer (Flash EA 1500; Thermo Finnigan,
222 Germany) coupled with an isotope ratio mass spectrometer (IRMS Delta^{plus}, Thermo
223 Finnigan, Germany). Briefly, this technique measures the ¹³C/¹²C ratio of total carbon of
224 the dried sample as follows: in a continuous helium flow, the sample is oxidized at 1000
225 °C in the presence of O₂ and catalysts; the resulting CO₂ is separated from the other
226 combustion products and transferred by the helium flow to a gas source, magnetic
227 sector, triple collector mass spectrometer. The latter determines the ¹³C/¹²C ratio of
228 CO₂-carbon. The stable carbon isotope composition is conventionally expressed as δ¹³C
229 values according to the formula:

$$\delta^{13}\text{C} \text{ ‰} = \left[\frac{(^{13}\text{C}/^{12}\text{C})_{\text{Sample}}}{(^{13}\text{C}/^{12}\text{C})_{\text{VPDB}}} - 1 \right] \times 1000$$

230 where VPDB is the Vienna Pee Dee Belemnite standard.

231 International Atomic Energy Agency (IAEA)-CH-7 polyethylene (δ¹³C = -32.2‰)
232 and IAEA-CH-6 sucrose were used as the calibration standard and control, respectively
233 [53]. The latter yielded a mean value of -10.5‰. The δ¹³C and carbon content of the
234 samples were corrected for the contribution of carbon in the tin capsules. The δ¹³C
235 standard deviations were determined from replicated measurements of the IAEA-CH-6
236 standard and were ± 0.2‰, ± 0.2‰, ± 0.4‰, and ± 0.7‰ for samples containing 20, 10,

237 5, and 2 $\mu\text{g C}$, respectively. The precision on the carbon content (precision on the
238 absolute amount of carbon analyzed) was $\pm 0.1 \mu\text{g C}$.

239 2.4.2. EA-AixMICADAS

240 Direct radiocarbon measurement of the CO_2 gas was carried out, after combustion,
241 using an elemental analyzer (EA) coupled to the gas interface system (GIS) of the
242 AixMICADAS system [48]. Briefly, the main characteristic of the EA is that it works
243 with a combustion tube filled with tungsten oxide heated to $1050 \text{ }^\circ\text{C}$ to allow the
244 introduction of silver boats containing the sample material. The purified extracts were
245 recovered in ultrapure water without acidification, transferred into silver capsules (4
246 $\text{mm} \times 8 \text{ mm}$, Elemental Microanalysis Ltd), and dried at $80 \text{ }^\circ\text{C}$ on a hotplate under a N_2
247 stream. The silver capsules were baked at $800 \text{ }^\circ\text{C}$ for 3 h prior to use to eliminate any
248 organic contamination [54,55]. The CO_2 produced by the EA is captured in the zeolite
249 trap inside the GIS. The CO_2 is then released by heating the zeolite trap to $450 \text{ }^\circ\text{C}$ and is
250 mixed inside the syringe with a helium flow in order to obtain 5% CO_2 in the gas
251 mixture, which is sputtered into the ion source. The CO_2 is injected from the GIS into
252 the ion source through a small fused silica capillary continuously fed by the syringe,
253 which is driven by a stepping motor controlled by the GIS software. A carbon flow of
254 $2.80 \mu\text{g C min}^{-1}$ keeps the total pressure constant inside the syringe (filled to 1300
255 mbar), allowing the ion source to produce stable currents. The tuning procedure and
256 main operation parameters used in the gas configurations are described in the literature
257 [48]. The measurements were normalized with the oxalic acid 2 standard ($\sim 100 \mu\text{g C}$;
258 OxA2 SRM 4990 C, National Institute of Standards and Technology) and corrected for
259 blanks using phthalic anhydride acid ($F^{14}\text{C} = 0.0027$; $n = 3$) prepared from the same
260 protocol as that used for OxA2 (i.e. silver capsules measured by EA-GIS).

261 The samples were blank corrected with procedural blanks of the same size (section
262 3.3) and a conservative uncertainty of 30% of the blank value was propagated in the
263 final error calculation. The samples were in the size range 50–150 $\mu\text{g C}$, which
264 translates to a precision of $\sim 1\%$ for a modern sample. However, samples down to 10 μg
265 C could be measured with less precision. The accuracy of ^{14}C measurements of small
266 samples ($< 100 \mu\text{g C}$) with the gas ion source of AixMICADAS has been tested with
267 numerous measurements on various standards (NIST 4990C, IAEA-C1, IAEA-C2, in-
268 house carbonate standards) [54,55]. For example, the analysis of oxalic acid NIST
269 4990C was replicated 132 times over 2.5 years, giving an average $F^{14}\text{C}$ of 1.3403 and a
270 standard deviation (SD) of 0.0078 (i.e. 6%). This arithmetic mean and its associated
271 error (std error = 0.0007) are compatible with the weighted mean (1.3405) and the
272 weighted error (0.0008), and closely agree with the NIST reference value of $1.3407 \pm$
273 0.0005.

274 The ^{14}C analyses were reported as $\Delta^{14}\text{C}$ corrected for decay [56,57] according to the
275 formula:

$$\Delta^{14}\text{C} \text{ ‰ (corrected for decay)} = \left(\frac{A_{SN} e^{\lambda_C (1950 - x)}}{A_{ON}} - 1 \right) \times 1000$$

276 where A_{SN} is the normalized sample activity, A_{ON} is the normalized standard activity,
277 x is the year of formation or growth, and $\lambda_C = (1/8267) \text{ yr}^{-1}$.

278 2.5. Identification of purified monosaccharides

279 The identification of the isolated purified monosaccharides was checked with Liquid
280 Chromatography coupled with Time-of-Flight Mass Spectrometry (LC-Q-TOF-MS)
281 Agilent 6500 system. The chromatographic separation was performed with a Luna
282 HILIC column (100 mm \times 2.00 mm I.D., 3 μm particle size; Phenomenex). The mobile
283 phase was ultrapure water with 13 mM $\text{CH}_3\text{COONH}_4$ (A) and acetonitrile (LC-MS

284 grade) with 13 mM CH₃COONH₄ (B) and sugars were eluted isocratically (20% A and
285 80% B). The flow rate and the column temperature were set at 200 $\mu\text{L min}^{-1}$ and 25 $^{\circ}\text{C}$,
286 respectively for the whole run. Monosaccharides were injected without prior
287 derivatization and ionized in the ESI positive mode. The main ion source parameters
288 were optimized as follows: source temperature 350 $^{\circ}\text{C}$, sheath gas temperature 350 $^{\circ}\text{C}$,
289 gas flow 11 L min^{-1} , and drying gas at 8 L min^{-1} . The MS scan was 50 – 1700 m/z, and
290 the scan rate was 1 spectra s^{-1} . The capillary voltage and the nozzle voltage were set at
291 4000 V and 500 V, respectively. Samples and standards were diluted in acetonitrile
292 before injection.

293 **3. Results and discussion**

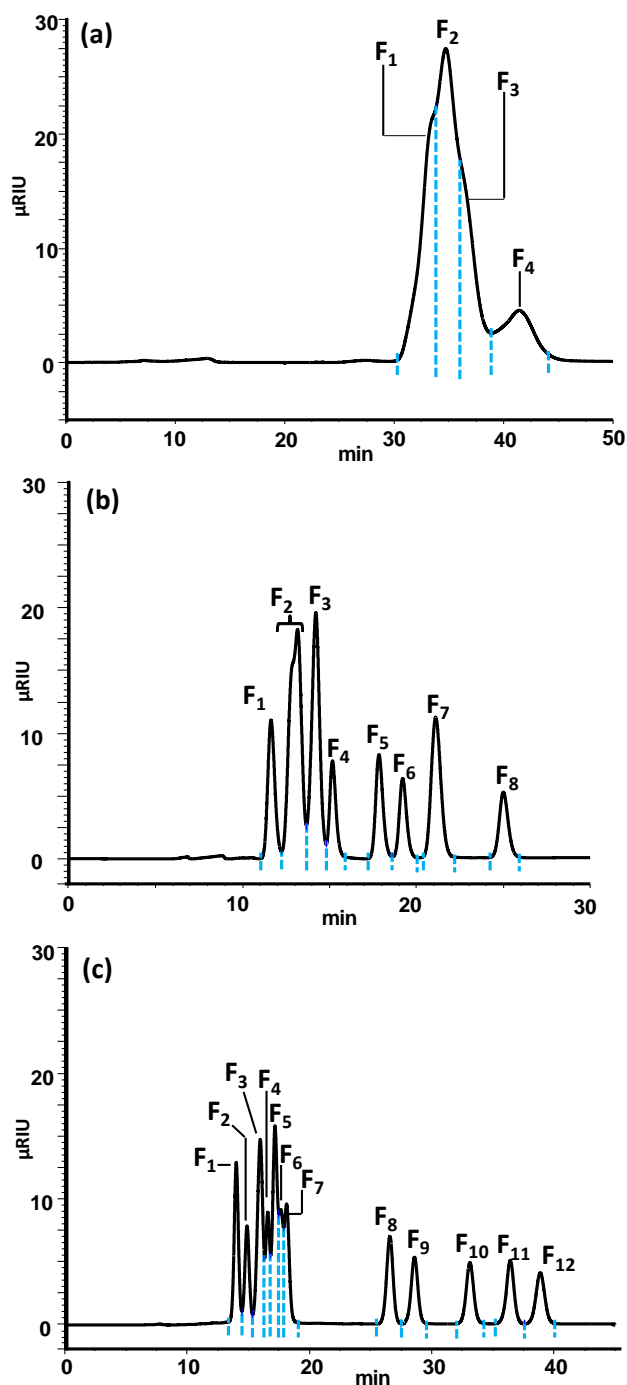
294 *3.1. Cation-exchange column selection and purification procedure*

295 Cation-exchange chromatography allows the separation of poly-, oligo-, and
296 monosaccharides based on their degree of polymerization [45,58]. The chromatographic
297 resolution and selectivity can be modulated by changing the cation-exchange column.
298 The separation mechanism is based on the strength of the complex formed between the
299 hydroxyl groups of the carbohydrate and the metal (e.g. K⁺, Na⁺, Pb²⁺, Ca²⁺, Cd²⁺, and
300 Cu²⁺).

301 In this study, Na⁺, Ca²⁺, and Pb²⁺ columns were selected for optimum purification of
302 the set of studied carbohydrates. The Na⁺ column is ideal to separate polysaccharides
303 from oligosaccharides and monosaccharides, whereas the Ca²⁺ and Pb²⁺ columns
304 provide further and complementary separation among the different monosaccharides
305 (e.g. neutral monosaccharides, alditols, anhydrosugars; Fig. 1 a-c). Compared to NH₂⁻
306 columns (also employed for sugar preparative chromatography), Na⁺, Ca²⁺, and Pb²⁺
307 columns have the advantage of running with ultrapure water as eluent instead of
308 acetonitrile. This considerably reduces the organic carbon contamination delivered by

309 the eluent, while ultrapure water is easily removed by evaporation with a minimum
310 organic carbon background left behind.

311 Because carbohydrates in environmental samples can also be polymers
312 (polysaccharides and oligosaccharides) and acid hydrolysis is not always 100%
313 effective [59], an initial purification on a Na^+ column was necessary to separate the
314 polymers from the monosaccharides [60]. The next step was the sequential purification
315 of the monosaccharides on the Ca^{2+} , Pb^{2+} and again, when necessary, on the Ca^{2+}
316 columns. This provided further and complementary separation among the different
317 monosaccharides (e.g. neutral monosaccharides, alditols, anhydrosugars; Fig. 1 b-c)
318 [61]. In summary the purification procedure flowchart proposed in this study is: $\text{Na}^+ \rightarrow$
319 $\text{Ca}^{2+} \rightarrow \text{Pb}^{2+} \rightarrow \text{Ca}^{2+}$.



320

321 **Fig. 1.** Chromatogram of a standard monosaccharide mixture (1 mM each): (a) Na^+
 322 column: F_1 (glucose + rhamnose + mannitol)/ F_2 (xylitol + sorbitol + fructose + mannose
 323 + galactose + xylose)/ F_3 (fucose + arabinose + galactosan)/ F_4 (levoglucosan +
 324 mannosan); (b) Ca^{2+} column: F_1 (glucose)/ F_2 (xylose + galactose + mannose +
 325 rhamnose)/ F_3 (fucose + fructose + arabinose)/ F_4 (galactosan)/ F_5 (mannitol)/ F_6
 326 (levoglucosan)/ F_7 (sorbitol + xylitol)/ F_8 (mannosan); and (c) Pb^{2+} column: F_1
 327 (glucose)/ F_2 (xylose)/ F_3 (galactose + rhamnose)/ F_4 (galactosan)/ F_5 (arabinose +

328 fucose)/F₆ (mannose)/F₇ (fructose)/F₈ (mannitol)/F₉ (levoglucosan)/F₁₀ (xylitol)/F₁₁
329 (sorbitol)/F₁₂ (mannosan). Dashed vertical lines correspond to the duration of the eluted
330 compound(s) and were used as the starting and ending points of peak collection by the
331 fraction collector.

332

333 *3.2. Monosaccharide standards purification and recovery yields*

334 The analytical procedure flowchart established in the previous section was tested on
335 monosaccharide standards (neutral monosaccharides, alditols, and anhydrosugars; initial
336 concentration of 50 μM) to evaluate the separation and peak isolation of the single
337 monosaccharides. The monosaccharide standards were sequentially purified on Ca²⁺ and
338 Pb²⁺ columns and if necessary, again on a Ca²⁺ column. Note that for the purpose of this
339 exercise the Na⁺ column was not included because the polysaccharides and
340 oligosaccharides were not considered in the standard (section 3.1).

341 The first separation was achieved on a Ca²⁺ column (Fig. S2 a) and resulted in eight
342 peaks corresponding to fractions F₁–F₈, which were collected into 6 mL pre-combusted
343 (450 °C, 6 h) glass tubes. The obtained results indicated that at this stage of the
344 purification process only the F₈ fraction (e.g. mannosan) was pure because it was eluted
345 significantly after the other monosaccharides (Fig. S2 a). Therefore, this
346 monosaccharide was not purified further. The collected fractions F₁–F₇ were freeze
347 dried, redissolved into 300 μL ultrapure water, and injected individually into the Pb²⁺
348 column (Fig. S2 b). It is worth noting that fractions in the time periods between the two
349 adjacent peaks were also collected and their purity was checked after injection into the
350 Pb²⁺ column. The monosaccharide(s), if any, obtained in such a way was (were) further
351 pooled with fraction(s) that contained the same monosaccharide to increase its recovery.
352 Following the second purification, 10 peaks were obtained corresponding to fractions

353 F₁–F₁₀. The last purification was performed on a Ca²⁺ column to ensure the collection of
354 ultrapure monosaccharide targets (Fig. S2 c).

355 The obtained results revealed that the recovery yields after three successive
356 purifications (Ca²⁺ → Pb²⁺ → Ca²⁺) of the standard mixture ranged from 12.38 ± 0.01%
357 to 36.32 ± 0.02% (n = 3), with the highest values observed for glucose, mannosan,
358 levoglucosan, and mannitol and the lowest for arabinose (Table S2). Notably, for
359 environmental sample analysis (section 3.5), the monosaccharides xylose, fucose, and
360 rhamnose were also included in the standard (in total 14 monosaccharides) despite the
361 fact that their recovery yield was not estimated via this exercise.

362 3.3. Chromatographic system blanks and background isotopic signature

363 The blanks were run on the HPLC-RI system with ultrapure water and the amount of
364 carbon released from the chromatographic columns (column bleeding) and isotopic
365 signature were evaluated (Table 1). Column blanks were recorded during the whole run
366 for each column: 50 min for the Na⁺ column, 30 min for the Ca²⁺ column, and 45 min
367 for the Pb²⁺ column. Subsequently, the amount of carbon released from these three
368 columns was measured via EA-IRMS. The obtained values were significantly close for
369 the Ca²⁺ and Pb²⁺ columns (4.84 ± 0.25 and 2.80 ± 0.21 µg, respectively), while those of
370 the Na⁺ column were much higher (28.64 ± 1.57 µg). Despite these differences, all the
371 blanks resulted in a similar δ¹³C signature ranging from -28.4 ± 0.4 to -27.8 ± 0.4‰
372 (Table 1).

373 The next step was to estimate the total carbon release after sequential purification on
374 the Na⁺ → Ca²⁺ → Pb²⁺ → Ca²⁺ columns. The obtained results indicated that the
375 purification procedure produced a blank that contained 19.76 ± 1.80 µg carbon (Table
376 1) with a δ¹³C value of -27.9 ± 1.1‰; these results were similar to those observed for
377 each column. Blanks corresponding to the collection time window of the three

378 monosaccharides (glucose, galactose, and levoglucosan) after $\text{Na}^+ \rightarrow \text{Ca}^{2+} \rightarrow \text{Pb}^{2+} \rightarrow$
379 Ca^{2+} purification were also run. The respective carbon inputs and the $\delta^{13}\text{C}$ signatures
380 after $\text{Na}^+ \rightarrow \text{Ca}^{2+} \rightarrow \text{Pb}^{2+} \rightarrow \text{Ca}^{2+}$ purification were $0.58 \pm 0.004 \mu\text{g}$ and $-24.4 \pm 2.9 \text{‰}$
381 for glucose and $0.54 \pm 0.15 \mu\text{g}$ and $-26.7 \pm 1.5\text{‰}$ for levoglucosan (Table 1).

382 Because of the elevated cost of radiocarbon analysis, radiocarbon blanks were only
383 run for the collection time trap of the three monosaccharides (glucose, galactose and
384 levoglucosan) measured in this study. Moreover, as the amount of carbon delivered for
385 the whole purification procedure ($\text{Na}^+ \rightarrow \text{Ca}^{2+} \rightarrow \text{Pb}^{2+} \rightarrow \text{Ca}^{2+}$ columns) for each of the
386 these monosaccharides was too small for a reliable $\Delta^{14}\text{C}$ measurement, phthalic acid
387 (^{14}C free blank sample) was added to the final collected blank and the sample was
388 processed as the monosaccharide sample (i.e. transferred into Ag capsules with
389 ultrapure water and combusted by the EA coupled to the gas interface of
390 AixMICADAS). The amount of phthalic acid was adjusted according to the size of the
391 sample to correct for constant contamination offsets. The results revealed that the
392 radiocarbon blanks exhibited values ranging from -988 to -986‰ (Table 1).

393 These $\Delta^{14}\text{C}$ values are slightly higher than those observed for the phthalic acid
394 samples ($\approx -997\text{‰}$) measured directly after addition into the silver capsules (i.e. without
395 any transfer from the collection tube to the silver cups). This suggests that little
396 exogenous carbon was added to the sample from HPLC purification (column bleeding
397 and organic residues), glassware contamination (collection vials, Pasteur pipets) and
398 airborne particle deposition during sample collection and transfer. Moreover, the $\Delta^{14}\text{C}$
399 values ($-989.7 \pm 3.5\text{‰}$) and carbon amounts ($0.52 \pm 0.34 \mu\text{g C}$) of the ultrapure water
400 samples (10 mL corresponding to ~ 10 times the volume of the collection window of a
401 pure monosaccharide) indicated that the addition of exogenous carbon from the eluent
402 was also negligible.

403 **Table 1.** Carbon content (μg), $\delta^{13}\text{C}$ (‰) and $\Delta^{14}\text{C}$ (‰) values of the procedural blanks. Phthalic
 404 acid was added to the collected time window of the three monosaccharide samples and the
 405 ultrapure water sample to make the measurement feasible. The mass of phthalic acid was
 406 adjusted according to the sample mass of the respective time window of the examined
 407 environmental samples.

408

Blank	Carbon \pm SD	$\delta^{13}\text{C} \pm$ SD	$\Delta^{14}\text{C} \pm$ SD
Na^+ column ($n = 3$) *	28.64 ± 1.57	-28.3 ± 0.8	ND
Ca^{2+} column ($n = 3$) *	4.84 ± 0.25	-28.4 ± 0.4	ND
Pb^{2+} column ($n = 3$) *	2.80 ± 0.21	-27.8 ± 0.4	ND
$\text{Na}^+ \rightarrow \text{Ca}^{2+} \rightarrow \text{Pb}^{2+} \rightarrow \text{Ca}^{2+}$ columns ($n = 3$)	19.76 ± 1.80	-27.9 ± 1.1	ND
Retention time window of glucose ($n = 3$) **	0.58 ± 0.00	-24.4 ± 2.9	$-986.2 \pm 5.8^{\S}$
Retention time window of galactose ($n = 2$) **	$< 2 \pm 2.0^{\dagger}$	ND	-988.2 ± 3.1
Retention time window of levoglucosan ($n = 3$) **	0.54 ± 0.15	-26.7 ± 1.5	$-988.2 \pm 0.9^{\ddagger}$
Ultrapure water ($n = 3$)	0.52 ± 0.34	-21.9 ± 5.9	-989.7 ± 3.5

409

410

411

412

413

414

415

416

ND: Not determined

* Measured for the whole HPLC -RI run time for each column (Table S1)

** Measured for the whole purification procedure ($\text{Na}^+ \rightarrow \text{Ca}^{2+} \rightarrow \text{Pb}^{2+} \rightarrow \text{Ca}^{2+}$)

$\S n = 4$

\dagger Measured with EA-AixMICADAS

$\ddagger n = 2$

417 Despite the significantly low amount of contaminants ($< 1\%$ for both the glucose and
 418 levoglucosan samples from the estimated carbon content of the retention time window)
 419 and the low $\Delta^{14}\text{C}$ procedural blanks, the results presented in this study were blank
 420 corrected. Finally, it is worth noting that the direct combustion of the small silver cups
 421 via an elemental analyzer allows a low background (equivalent age of 46 000 yr BP)
 422 and is therefore a good alternative to the time-consuming conventional method based on
 423 purification with a vacuum line.

424 Overall, the above results clearly suggest that the proposed purification procedure
 425 does not induce any significant contamination in the samples or affect their isotopic
 426 signature.

427 *3.4. Hydrolysis effects*

428 The marine sample was submitted to hydrolysis (1 M HCl) prior to its
429 chromatographic purification (Section 2) to release the monosaccharides from the
430 biopolymer macrostructure. Moreover, additional experiments were performed on the
431 standard mono- and polysaccharides to investigate whether the hydrolysis conditions
432 affect the isotopic composition of the released monosaccharides. The three levoglucosan
433 standard solutions (90 $\mu\text{g C}$ each) presented similar $\delta^{13}\text{C}_{\text{levo}}$ values, namely $-11.2 \pm$
434 0.2‰ ($n = 3$) and $-11.2 \pm 0.1\text{‰}$ ($n = 3$) before and after hydrolysis, respectively.
435 Similar results were obtained by Wang et al. [19] for the glucose standard ($\delta^{13}\text{C}_{\text{glc}} =$
436 -9.8‰ and $\delta^{13}\text{C}_{\text{glc}} = -9.9\text{‰}$ before and after processing, respectively); however their
437 study included additional purification steps comprising anion and cation-exchange
438 resins.

439 In another set of experiments a polysaccharide standard (laminarin) containing
440 glucose units was submitted to acid hydrolysis and the isotopic signature of the released
441 glucose was compared to that of the original laminarin. The results indicated that
442 glucose and laminarin exhibited similar isotopic signatures in terms of $\delta^{13}\text{C}$ ($\delta^{13}\text{C}_{\text{glc}} =$
443 -10.4‰ and $\delta^{13}\text{C}_{\text{lam.}} = -13.0\text{‰}$; $n = 1$) and $\Delta^{14}\text{C}$ ($\Delta^{14}\text{C}_{\text{glc}} = -85.4\text{‰}$ and $\Delta^{14}\text{C}_{\text{lam.}} =$
444 -84.90‰ ; $n = 1$) indicating few differences between the isotopic composition of the
445 original polysaccharide and its monomeric constituent (Repeta; unpublished results).

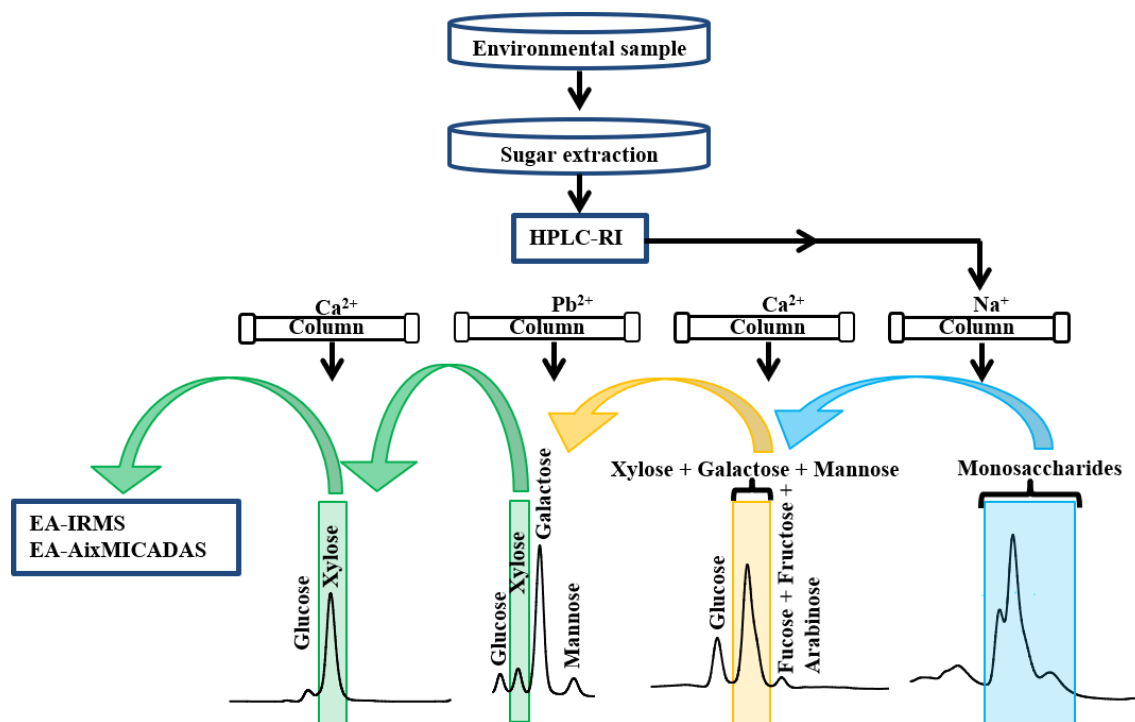
446

447 *3.5. Application to environmental samples*

448 The purification procedure, including sample preparation, employed in this study is
449 briefly summarized in Fig. 2. Two distinct environmental samples, namely, a marine
450 POM and a TSP sample were considered. The choice of samples was made with respect

451 to the opportunities and the logistics set to obtain them but more importantly of their
452 high carbohydrate content.

453



454

455 **Fig. 2.** Procedural flowchart of this study with a simplified example of the purification
456 of xylose isolated from the marine particulate organic matter (POM) sample. The last
457 purification of xylose on the Ca²⁺ was obtained after pooling the xylose fraction
458 collected from the Pb²⁺ column and the xylose purified from the adjacent fractions.

459

460 3.5.1. Marine POM

461 The hydrolyzed marine sample was processed on a Na⁺ column and the collected
462 fractions (F₃–F₆), corresponding to the monosaccharides, were further purified on
463 Ca²⁺ → Pb²⁺ → Ca²⁺ columns (Fig. 3). The results indicated that after four sequential
464 purifications the major monosaccharides obtained were: galactose (368 μg), glucose
465 (273 μg), mannose (65 μg), xylose (38 μg), and fucose/arabinose (16 μg). It is worth
466 noting that levoglucosan (1.8 μg) and mannosan (1.5 μg) were also collected for the

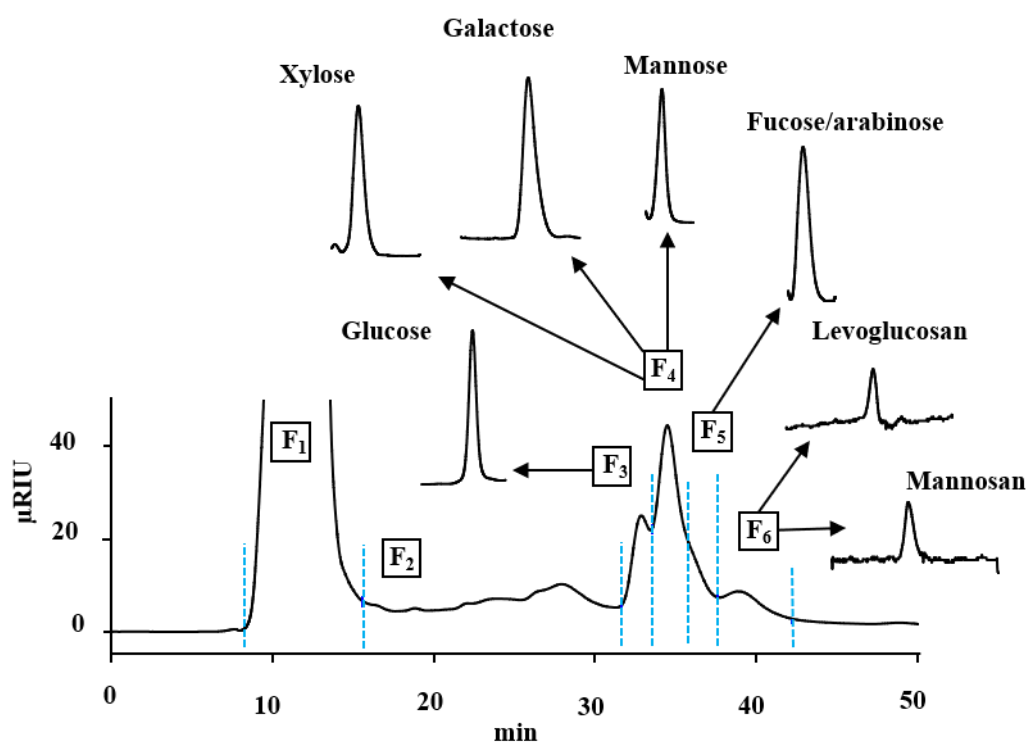
467 first time from marine POM; however, in very low amounts. The presence of the
468 abovementioned anhydrosugars in the hydrolyzed marine sample was also confirmed by
469 high-performance anion-exchange chromatography (Nouara et al., *submitted*). Finally,
470 although rhamnose and galactosan were detected in the marine POM sample they
471 yielded very small recovered amounts ($< 0.5 \mu\text{g}$), which were insufficient for isotopic
472 measurement.

473 The results revealed that the marine POM sample exhibited a $\delta^{13}\text{C}$ value of $-19.6 \pm$
474 0.6‰ which is typical of marine origin and consistent with the $\delta^{13}\text{C}$ values reported for
475 the surface coastal sinking POM (range: -23 to -20‰) [18,62]. The $\delta^{13}\text{C}$ signature of
476 the POM hydrophilic extract (fraction comprising most of the hydrophilic components
477 of the sample including monosaccharides) was slightly enriched ($-17.2 \pm 0.5\text{‰}$)
478 compared to that of the bulk POM and agreed well with the $\delta^{13}\text{C}$ values recorded for
479 glucose, galactose, mannose, xylose, and fucose/rhamnose (-18.5 to -16.8‰ ; Table 2).

480 The $\delta^{13}\text{C}$ signature recorded for these individual monosaccharides agrees well with
481 the isotopic values measured for the individual monosaccharides in marine high-
482 molecular-weight dissolved organic matter (HMWDOM) [27], and thereby pointing
483 toward a marine origin. The slight depletion of the $\delta^{13}\text{C}$ values of the bulk POM relative
484 to its individual carbohydrate component may be due to the presence of other organic
485 compounds (e.g. amino acids and lipids) in the sample, which may have a lighter stable
486 carbon isotope signature than that observed for carbohydrates [20,22]. Regardless,
487 further molecular level isotopic analysis on individual amino acids and/or lipids is
488 warranted to test this hypothesis.

489 On the other hand, the levoglucosan (-27.2‰) and mannosan (-26.2‰) isotopic
490 signatures exhibited depleted $\delta^{13}\text{C}$ values when compared to those of the other
491 monosaccharides, indicating the different origin of these two monosaccharides (Table

492 2). Indeed, these sugars are well known tracers of terrestrial biomass burning processes
 493 [39], and thus their presence in marine POM indicates an external terrestrial input
 494 probably via atmospheric deposition [5,10] from C3 land plant tissue ($\delta^{13}\text{C}$: -32 to
 495 -20% ; mean: -27% [63]). The presence of levoglucosan and mannosan in the POM
 496 sample is not surprising since the sampling site was located a few kilometers offshore
 497 from the Lima area (section 2.2).



498

499 **Fig. 3.** Chromatogram of a marine particulate organic matter (POM) sample on a Na^+
 500 column (F₁: polysaccharides; F₂: oligosaccharides; F₃: glucose, rhamnose; F₄: xylose,
 501 galactose, and mannose; F₅: fucose + arabinose, and galactosan; F₆: mannosan and
 502 levoglucosan). The final purified compounds (after $\text{Na}^+ \rightarrow \text{Ca}^{2+} \rightarrow \text{Pb}^{2+} \rightarrow \text{Ca}^{2+}$
 503 purification) are also indicated with arrows.

504

505 The radiocarbon results of this study indicated that relatively to its hydrophilic
 506 fraction ($\Delta^{14}\text{C} = 124 \pm 5\%$), the marine POM sample was depleted ($\Delta^{14}\text{C} = 28 \pm 8\%$).

507 This agrees very well with previous investigations, which have reported similar results
 508 for a wide variety of environmental samples comprising sediments, sinking POM,
 509 planktons [19,64] including riverine, and marine HMWDOM [22,65]. Intermediate
 510 radiocarbon values were recorded for glucose and galactose ($\Delta^{14}\text{C}_{\text{glc}} = 43\text{‰}$ and $\Delta^{14}\text{C}_{\text{gal}}$
 511 $= 19\text{‰}$; Table 2) and are consistent with the radiocarbon monosaccharide signature
 512 reported for surface marine HMWDOM [27].

513

514 **Table 2.** $\delta^{13}\text{C}$ (‰) \pm SD and $\Delta^{14}\text{C}$ (‰) \pm SD values of the examined environmental samples.
 515 The $\Delta^{14}\text{C}$ values of galactose, glucose and levoglucosan are blank-corrected.

Sample	Bulk OM [§]	Hydrophilic OM [§] extract	Pure monosaccharides		
	$\delta^{13}\text{C} / \Delta^{14}\text{C}$ (<i>n</i> = 3)	$\delta^{13}\text{C} / \Delta^{14}\text{C}$ (<i>n</i> = 3)		$\delta^{13}\text{C}$ (<i>n</i> = 3)	$\Delta^{14}\text{C} \pm 1 \sigma$
POM	-19.6 \pm 0.6 / 28 \pm 8	-17.2 \pm 0.5 / 124 \pm 5	Mannose	-17.6 \pm 0.9	-
			Xylose	-16.8 \pm 0.2	-
			Fuc./Ara. ^{§§}	-18.5 \pm 0.5	-
			Galactose	-16.9 \pm 0.1	18.9 \pm 16.3 (<i>n</i> = 3)**
			Glucose	-17.6 \pm 0.1	43.3 \pm 9.9 (<i>n</i> = 1)
			Levoglucosan	-27.2 *	-
			Mannosan	-26.2 *	-
TSP	-25.9 \pm 0.0 / -175 \pm 5	-24.8 \pm 0.1 / -64 \pm 13	Glucose	-25.1 \pm 0.1	-
			Fructose	-25.3 \pm 0.3	-
			Levoglucosan	-25.0 \pm 0.4	33.0 \pm 9.7 (<i>n</i> = 1)
			Mannosan	-25.7 \pm 0.5	-
			Mannitol	-26.4 *	-

516 [§] Organic matter

517 ^{§§} Fucose / Arabinose

518 * *n* = 1

519 ** $\Delta^{14}\text{C} \pm$ SD

520

521 Overall, the above radiocarbon data indicate a modern age for the purified
 522 monosaccharides that further support the hypothesis that these monosaccharides are
 523 incorporated into a common family of polysaccharides (acylpolysaccharides) present in
 524 all terrestrial and aquatic ecosystems [66,67]. Nevertheless, more $\Delta^{14}\text{C}$ data on the

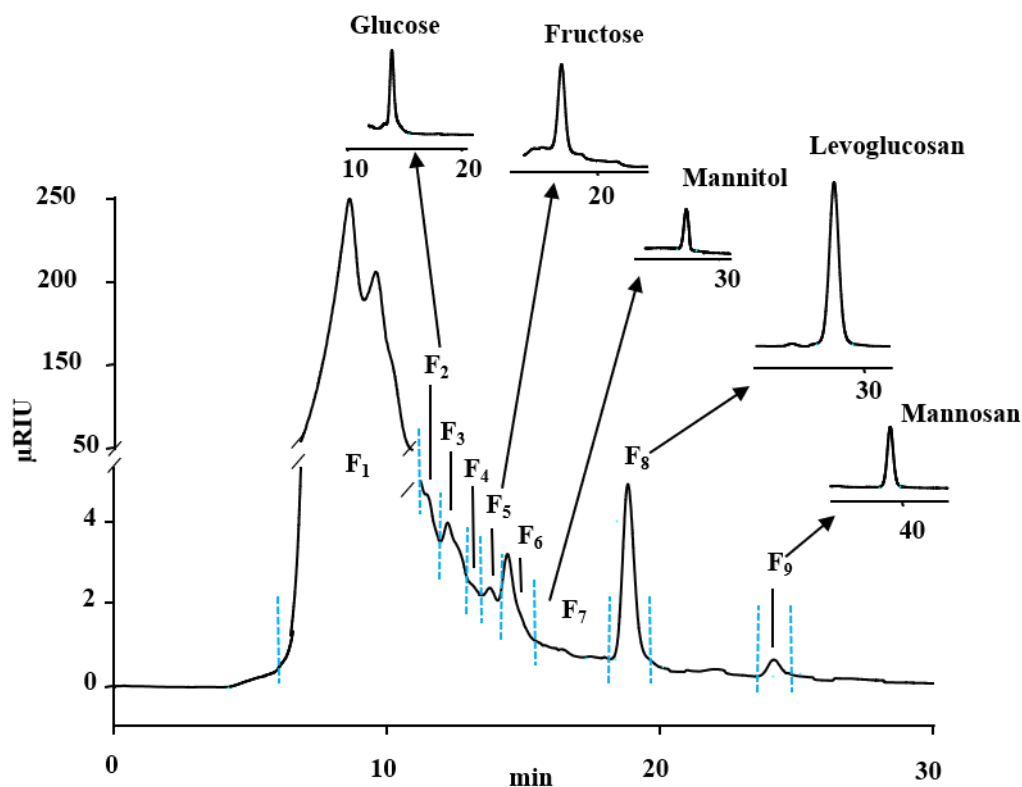
525 individual monosaccharides including other environmental matrices (e.g. sediments, and
526 riverine POM and DOM) are warranted before any generalizations can be made.

527

528 3.5.2. TSP

529 The purification of the atmospheric sample was performed, without prior processing,
530 on the Na⁺ column. This was due to the low complexity of the sample and to avoid
531 further possible losses and contamination that may occur during additional
532 manipulation. The purification was conducted in a Ca²⁺ column, followed by a Pb²⁺
533 column and again by a Ca²⁺ column (Fig. 4). The obtained results indicated that after
534 three purifications the major monosaccharides obtained were: levoglucosan (134 µg),
535 fructose (40 µg), mannosan (38 µg), glucose (36 µg), and mannitol (4 µg). The
536 abundance of these monosaccharides is in agreement with the results generally reported
537 for PM₁₀ particles [5,10]. Similar to the abovementioned results galactose, arabinose
538 and galactosan were detected in the TSP sample. However, these were present in very
539 low amounts (< 0.5 µg) and no isotopic measurements were performed.

540 The δ¹³C value recorded for the TSP sample (−25.9 ± 0.0‰) was similar to that of its
541 hydrophilic extract (−24.8 ± 0.1‰) and within the range of that of the isolated
542 monosaccharides (−26.4 to −25.0‰; Table 2). These results reflect a dominant
543 terrestrial origin from C3 vegetation and/or microorganisms, including fungal spores
544 [6,37]. The δ¹³C values of levoglucosan and mannosan were in agreement with the
545 values reported by Sang et al. [25] for hardwood and stalk plant combustion. The δ¹³C
546 values reported in this study are also in good agreement with those measured for *n*-
547 alkanes (C₂₃–C₃₃: −26.7 to −28.5‰), *n*-alkanols (C₂₂–C₃₂: −23.9 to −30.4‰), and long-
548 chain *n*-alkanoic acids (C₂₂–C₃₂: −22.6 to −27.4‰) in the north western African dust
549 over the Atlantic Ocean [41].



550

551 **Fig. 4.** Chromatogram of the total suspended atmospheric particles (TSP) on a Ca^{2+}
 552 column (F_1 : polymer; F_2 : glucose; F_3 : unknown; F_4 : galactose; F_5 : arabinose and
 553 fructose; F_6 : unknown and galactosan; F_7 : mannitol; F_8 : levoglucosan; F_9 : mannosan).
 554 The final purified compounds (after $\text{Ca}^{2+} \rightarrow \text{Pb}^{2+} \rightarrow \text{Ca}^{2+}$ purification) are also indicated
 555 with arrows.

556

557 The radiocarbon signature of the TSP sample (Table 2) indicated that the bulk
 558 sample was highly depleted ($-175 \pm 5\%$; 1545 yr) relative to its hydrophilic component
 559 ($-64 \pm 13\%$; 530 yr). This is consistent with the characteristics already observed for the
 560 POM sample (section 3.5.1). The purified levoglucosan exhibited a modern radiocarbon
 561 age (33‰; Table 2), implying a very recent synthesis of this monosaccharide, which
 562 agrees with the radiocarbon signature of contemporary biosphere carbon ($\Delta^{14}\text{C} = 0$ to
 563 200‰) and concurs with the radiocarbon monosaccharide data of the marine POM
 564 sample. Although this result is a single and unique up-to-date measure of the $\Delta^{14}\text{C}$ of

565 levoglucosan, it can also explain, in part, the lack of stability of levoglucosan in the
566 atmosphere over time since this compound has a modern age [68,69]. The radiocarbon
567 signature of the TSP sample (1545 yr) relative to those of the purified water extract (530
568 yr) and levoglucosan (modern), may be due to the contribution of aged organic material
569 such as black carbon (>50,000 yr). This material is known to be ubiquitous in the
570 atmosphere as a result of fossil fuel emissions. This observation is further supported by
571 the location of the sampling site (Marseille, France), which is characterized by the high
572 influence from anthropogenic emissions and is in agreement with previous radiocarbon
573 data performed on fossil fuels, soot aerosols, and PM_{2.5} particles in other areas [70–72].
574 However, more TSP radiocarbon data in conjunction with compound specific
575 radiocarbon analyses (i.e. monosaccharides, lipids, polyaromatic hydrocarbons) are
576 required to confirm this hypothesis.

577

578 *3.6. Identification of purified monosaccharides: comparison with authentic* 579 *standards*

580 Isolated monosaccharides recovered after the whole extraction and purification
581 procedure were compared with authentic standards to check their purity. Depending on
582 the amount of carbon recovered and the number of subsequently performed replicate
583 EA-IRMS analysis, only three monosaccharides were further explored: levoglucosan,
584 glucose, and galactose. The results from this study indicated that the mass spectra of the
585 isolated monosaccharides well matched those of authentic standards (Table S3), as
586 revealed by liquid chromatography coupled with quadrupole time-of-flight mass
587 spectrometry (Q-TOF-LC/MS; Fig. S3). These results indicate that this proposed
588 approach is specific, valid and reliable.

589 **4. Conclusions and Outlook**

590 The approach presented herein proved to be a powerful and robust tool for $\delta^{13}\text{C}$ and
591 $\Delta^{14}\text{C}$ determination of individual carbohydrates in the environmental matrices. Briefly,
592 after four successive purifications on cation-exchange columns, the pure carbohydrates
593 were produced and further assessed by EA-IRMS and/or EA-AixMICADAS. Particular
594 attention was given to the procedural blanks, which were found to be extremely low
595 during the whole cleanup procedure (0.5 $\mu\text{g C}$ per carbohydrate collected).

596 The applicability of the proposed procedure was tested on two different
597 environmental samples comprising marine POM and TSP and the results revealed that
598 the isotopic compositions of the individual carbohydrates, in terms of $\delta^{13}\text{C}$, were in
599 good agreement with the data reported in the literature. Unfortunately, the $\Delta^{14}\text{C}$ values
600 for individual carbohydrates are scarce in literature and to the best of our knowledge,
601 only one study, on marine HMWDOM, has been reported to date. Therefore, we could
602 not directly compare the obtained results to $\Delta^{14}\text{C}$ values of similar samples.
603 Nevertheless, the obtained data suggested that the monosaccharides exhibit a modern
604 age, further implying the recent synthesis of these compounds and their rapid cycling.
605 Applying this method to a wide variety of environmental samples comprising marine
606 sediments, riverine organic matter, deep water HMWDOM, soils, and rain may
607 substantially help to improve the understanding of the carbohydrate dynamics and
608 organic matter cycling in all geochemical systems.

609 Finally, the overall approach highlights the high potential of preparative liquid
610 chromatography for application to the purification of specific compounds after selection
611 of the adequate column(s) for subsequent molecular-level isotopic measurements.
612 Moreover, future research employing two-dimensional cation-exchange
613 chromatography may prove to be a very useful tool to speed up the whole purification
614 procedure.

615

616 **Acknowledgments**

617 This research was funded by the projects AIOLOS, TRACFIRE (Labex OT-Med;
618 ANR-11-LABEX-0.061) and MANDARINE (grant No 2008-10372; Région Provence
619 Alpes Côte d'Azur). The project leading to this publication has received funding from
620 European FEDER Fund under project 1166-39417. The authors acknowledge the four
621 anonymous reviewers for valuable comments and fruitful discussions. A. Nouara was
622 supported by a Ph.D. grant from Aix-Marseille University.

623

624 **Appendix A. Supplementary data**

625 Supplementary data related to this article can be found at <https://doi.org/10.1016/j.aca>

626 **Table and Figure captions**

627 **Table 1.** Carbon content (μg), $\delta^{13}\text{C}$ (‰) and $\Delta^{14}\text{C}$ (‰) values of the procedural blanks.
628 Phthalic acid was added to the collected time window of the three monosaccharide
629 samples and the ultrapure water sample to make the measurement feasible. The mass of
630 phthalic acid was adjusted according to the sample mass of the respective time window
631 of the examined environmental samples.

632

633 **Table 2.** $\delta^{13}\text{C}$ (‰) \pm SD and $\Delta^{14}\text{C}$ (‰) \pm SD values of the examined environmental
634 samples. The $\Delta^{14}\text{C}$ values of galactose, glucose and levoglucosan are blank-corrected.

635

636 **Fig. 1.** Chromatogram of a standard monosaccharide mixture (1 mM each): (a) Na⁺
637 column: F₁ (glucose + rhamnose + mannitol)/F₂ (xylitol + sorbitol + fructose + mannose
638 + galactose + xylose)/F₃ (fucose + arabinose + galactosan)/F₄ (levoglucosan +
639 mannosan); (b) Ca²⁺ column: F₁ (glucose)/F₂ (xylose + galactose + mannose +
640 rhamnose)/F₃ (fucose + fructose + arabinose)/F₄ (galactosan)/F₅ (mannitol)/F₆
641 (levoglucosan)/F₇ (sorbitol + xylitol)/F₈ (mannosan); and (c) Pb²⁺ column: F₁
642 (glucose)/F₂ (xylose)/F₃ (galactose + rhamnose)/F₄ (galactosan)/F₅ (arabinose +
643 fucose)/F₆ (mannose)/F₇ (fructose)/F₈ (mannitol)/F₉ (levoglucosan)/F₁₀ (xylitol)/F₁₁
644 (sorbitol)/F₁₂ (mannosan). Dashed vertical lines correspond to the duration of the eluted
645 compound(s) and were used as the starting and ending points of peak collection by the
646 fraction collector.

647 **Fig. 2.** Procedural flowchart of this study with a simplified example of the purification
648 of xylose isolated from the marine particulate organic matter (POM) sample. The last
649 purification of xylose on the Ca²⁺ was obtained after pooling the xylose fraction
650 collected from the Pb²⁺ column and the xylose purified from the adjacent fractions.

651

652 **Fig. 3.** Chromatogram of a marine particulate organic matter (POM) sample on a Na⁺
653 column (F₁: polysaccharides; F₂: oligosaccharides; F₃: glucose, rhamnose; F₄: xylose,
654 galactose, and mannose; F₅: fucose + arabinose, and galactosan; F₆: mannosan and
655 levoglucosan). The final purified compounds (after Na⁺→Ca²⁺→Pb²⁺→Ca²⁺
656 purification) are also indicated with arrows.

657

658 **Fig. 4.** Chromatogram of the total suspended atmospheric particles (TSP) on a Ca²⁺
659 column (F₁: polymer; F₂: glucose; F₃: unknown; F₄: galactose; F₅: arabinose and
660 fructose; F₆: unknown and galactosan; F₇: mannitol; F₈: levoglucosan; F₉: mannosan).

661 The final purified compounds (after $\text{Ca}^{2+} \rightarrow \text{Pb}^{2+} \rightarrow \text{Ca}^{2+}$ purification) are also indicated
662 with arrows.

663

664 **References**

665 [1] J.I. Hedges, G.L. Cowie, J.E. Richey, P.D. Quay, R. Benner, M. Strom, B.R.
666 Forsberg, Origins and processing of organic matter in the Amazon River as
667 indicated by carbohydrates and amino acids, *Limnol. Oceanogr.* 39 (1994) 743–
668 761. doi:10.4319/lo.1994.39.4.0743.

669 [2] S. Opsahl, R. Benner, Characterization of carbohydrates during early diagenesis
670 of five vascular plant tissues, *Org. Geochem.* 30 (1999) 83–94.
671 doi:10.1016/S0146-6380(98)00195-8.

672 [3] C. Panagiotopoulos, D.J. Repeta, L. Mathieu, J.F. Rontani, R. Sempéré,
673 Molecular level characterization of methyl sugars in marine high molecular
674 weight dissolved organic matter, *Mar. Chem.* 154 (2013) 34–45.
675 doi:10.1016/j.marchem.2013.04.003.

676 [4] D.J. Repeta, Chemical characterization and cycling of dissolved organic matter,
677 in: D. A. Hansell and C. A. Carlson (Ed.), *Biogeochem. Mar. Dissolved Org.*
678 *Matter*, Elsevier Science, USA, 2015: pp. 21–63.

679 [5] C. Theodosi, C. Panagiotopoulos, A. Nouara, P. Zampas, P. Nicolaou, K.
680 Violaki, M. Kanakidou, R. Sempéré, N. Mihalopoulos, Sugars in atmospheric
681 aerosols over the Eastern Mediterranean, *Prog. Oceanogr.* 163 (2018) 70–81.
682 doi:10.1016/j.pocean.2017.09.001.

683 [6] P. Fu, K. Kawamura, M. Kobayashi, B.R.T. Simoneit, Seasonal variations of

- 684 sugars in atmospheric particulate matter from Gosan, Jeju Island: Significant
685 contributions of airborne pollen and Asian dust in spring, *Atmos. Environ.* 55
686 (2012) 234–239. doi:10.1016/j.atmosenv.2012.02.061.
- 687 [7] J.M. Oades, Soil organic matter and structural stability: mechanisms and
688 implications for management, *Plant Soil.* 76 (1984) 319–337.
- 689 [8] C. Panagiotopoulos, R. Sempéré, J. Para, P. Raimbault, C. Rabouille, B.
690 Charrière, The composition and flux of particulate and dissolved carbohydrates
691 from the Rhone River into the Mediterranean Sea, *Biogeosciences.* 9 (2012)
692 1827–1844. doi:10.5194/bg-9-1827-2012.
- 693 [9] J.D. Pakulski, R. Benner, Abundance and distribution of carbohydrates in the
694 ocean, *Limnol. Oceanogr.* 39 (1994) 930–940. doi:10.4319/lo.1994.39.4.0930.
- 695 [10] P. Fu, K. Kawamura, K. Miura, Molecular characterization of marine organic
696 aerosols collected during a round-the-world cruise, *J. Geophys. Res.* 116 (2011)
697 1–14. doi:10.1029/2011JD015604.
- 698 [11] R. Sempéré, M. Tedetti, C. Panagiotopoulos, B. Charriere, F. Van Wambeke,
699 Distribution and bacterial availability of dissolved neutral sugars in the South
700 East Pacific, *Biogeosciences.* 5 (2008) 1165–1173. doi:10.5194/bg-5-1165-2008.
- 701 [12] S.R. Beaupré, The Carbon Isotopic Composition of Marine DOC, in: D.A.
702 Hansell, C.A. Carlson (Eds.), *Biogeochem. Mar. Dissolved Org. Matter*, Second
703 Edi, Academic Press, Boston, 2015: pp. 335–368.
704 doi:https://doi.org/10.1016/B978-0-12-405940-5.00006-6.
- 705 [13] E.A. Hobbie, R.A. Werner, Intramolecular, compound-specific, and bulk carbon
706 isotope patterns in C₃ and C₄ plants: a review and synthesis, *New Phytol.* 161

- 707 (2004) 371–385. doi:10.1046/j.1469-8137.2004.00970.x.
- 708 [14] J. Hwang, E.R.M. Druffel, Carbon isotope ratios of organic compound fractions
709 in oceanic suspended particles, *Geophys. Res. Lett.* 33 (2006) 1–5.
710 doi:10.1029/2006GL027928.
- 711 [15] D. López-Veneroni, The stable carbon isotope composition of PM_{2.5} and PM₁₀
712 in Mexico City Metropolitan Area air, *Atmos. Environ.* 43 (2009) 4491–4502.
713 doi:10.1016/j.atmosenv.2009.06.036.
- 714 [16] C.P. Bataille, M. Mastalerz, B.J. Tipple, G.J. Bowen, Influence of provenance
715 and preservation on the carbon isotope variations of dispersed organic matter in
716 ancient floodplain sediments, *Geochemistry, Geophys. Geosystems.* 14 (2013)
717 4874–4891. doi:10.1002/ggge.20294.
- 718 [17] P.K. Zigah, E.C. Minor, H.A.N. Abdulla, J.P. Werne, P.G. Hatcher, An
719 investigation of size-fractionated organic matter from Lake Superior and a
720 tributary stream using radiocarbon, stable isotopes and NMR, *Geochim.*
721 *Cosmochim. Acta.* 127 (2014) 264–284. doi:10.1016/j.gca.2013.11.037.
- 722 [18] L.A. Roland, M.D. McCarthy, T. Guilderson, Sources of molecularly
723 uncharacterized organic carbon in sinking particles from three ocean basins: A
724 coupled $\Delta^{14}\text{C}$ and $\delta^{13}\text{C}$ approach, *Mar. Chem.* 111 (2008) 199–213.
725 doi:10.1016/j.marchem.2008.05.010.
- 726 [19] X.-C. Wang, E.R.M. Druffel, S. Griffin, C. Lee, M. Kashgarian, Radiocarbon
727 studies of organic compounds classes in plankton and sediment of the
728 northeastern Pacific Ocean, *Geochim. Cosmochim. Acta.* 62 (1998) 1365–1378.
729 doi:10.1016/S0016-7037(98)00074-X.

- 730 [20] J. Hwang, E.R.M. Druffel, Lipid-Like Material as the Source of the
731 Uncharacterized Organic Carbon in the Ocean?, *Science*. 299 (2003) 881–884.
732 doi:10.1126/science.1078508.
- 733 [21] X.-C. Wang, R.F. Chen, G.B. Gardner, Sources and transport of dissolved and
734 particulate organic carbon in the Mississippi River estuary and adjacent coastal
735 waters of the northern Gulf of Mexico, *Mar. Chem.* 89 (2004) 241–256.
736 doi:10.1016/j.marchem.2004.02.014.
- 737 [22] A.N. Loh, J.E. Bauer, E.R.M. Druffel, Variable ageing and storage of dissolved
738 organic components in the open ocean., *Nature*. 430 (2004) 877–881.
739 doi:10.1038/nature02780.
- 740 [23] B.E. Van Dongen, S. Schouten, J.S. Sinninghe Damsté, Carbon isotope
741 variability in monosaccharides and lipids of aquatic algae and terrestrial plants,
742 *Mar. Ecol. Prog. Ser.* 232 (2002) 83–92. doi:10.3354/meps232083.
- 743 [24] B. Glaser, Compound-specific stable-isotope ($\delta^{13}\text{C}$) analysis in soil science, *J.*
744 *Plant Nutr. Soil Sci.* 168 (2005) 633–648. doi:10.1002/jpln.200521794.
- 745 [25] X.F. Sang, I. Gensch, W. Laumer, B. Kammer, C.Y. Chan, G. Engling, A.
746 Wahner, H. Wissel, A. Kiendler-Scharr, Stable carbon isotope ratio analysis of
747 anhydrosugars in biomass burning aerosol particles from source samples,
748 *Environ. Sci. Technol.* 46 (2012) 3312–3318. doi:10.1021/es204094v.
- 749 [26] R. Zhu, Y.-S. Lin, J. Lipp, T.B. Meador, K.-U. Hinrichs, Optimizing sample
750 pretreatment for compound-specific stable carbon isotopic analysis of amino
751 sugars in marine sediment, *Biogeosciences*. 11 (2014) 4869–4880.
752 doi:10.5194/bg-11-593-2014.

- 753 [27] D.J. Repeta, L.I. Aluwihare, Radiocarbon analysis of neutral sugars in high-
754 molecular-weight dissolved organic carbon: Implications for organic carbon
755 cycling, *Limnol. Oceanogr.* 51 (2006) 1045–1053.
756 doi:10.4319/lo.2006.51.2.1045.
- 757 [28] D. Derrien, J. Balesdent, C. Marol, C. Santaella, Measurement of the $^{13}\text{C}/^{12}\text{C}$
758 ratio of soil-plant individual sugars by gas chromatography/combustion/isotope-
759 ratio mass spectrometry of silylated derivatives, *Rapid Commun. Mass Spectrom.*
760 17 (2003) 2626–2631. doi:10.1002/rcm.1269.
- 761 [29] M.A. Teece, M.L. Fogel, Stable carbon isotope biogeochemistry of
762 monosaccharides in aquatic organisms and terrestrial plants, *Org. Geochem.* 38
763 (2007) 458–473. doi:10.1016/j.orggeochem.2006.06.008.
- 764 [30] T.C.W. Moerdijk-Poortvliet, H. Schierbeek, M. Houtekamer, T. van Engeland,
765 D. Derrien, L.J. Stal, H.T.S. Boschker, Comparison of gas
766 chromatography/isotope ratio mass spectrometry and liquid
767 chromatography/isotope ratio mass spectrometry for carbon stable-isotope
768 analysis of carbohydrates, *Rapid Commun. Mass Spectrom.* 29 (2015) 1205–
769 1214. doi:10.1002/rcm.7217.
- 770 [31] C. Panagiotopoulos, R. Sempéré, Analytical methods for the determination of
771 sugars in marine samples : A historical perspective and future directions, *Limnol.*
772 *Oceanogr. Methods.* 3 (2005) 419–454. doi:10.4319/lom.2005.3.419.
- 773 [32] T.C.W. Moerdijk-Poortvliet, L.J. Stal, H.T.S. Boschker, LC/IRMS analysis: A
774 powerful technique to trace carbon flow in microphytobenthic communities in
775 intertidal sediments, *J. Sea Res.* 92 (2014) 19–25.
776 doi:10.1016/j.seares.2013.10.002.

- 777 [33] H.T.S. Boschker, T.C.W. Moerdijk-Poortvliet, P. van Breugel, M. Houtekamer,
778 J.J. Middelburg, A versatile method for stable carbon isotope analysis of
779 carbohydrates by high-performance liquid chromatography/isotope ratio mass
780 spectrometry., *Rapid Commun. Mass Spectrom.* 22 (2008) 3902–3908.
781 doi:10.1002/rcm.3804.
- 782 [34] A. Basler, J. Dyckmans, Compound-specific $\delta^{13}\text{C}$ analysis of monosaccharides
783 from soil extracts by high-performance liquid chromatography/isotope ratio mass
784 spectrometry, *Rapid Commun. Mass Spectrom.* 27 (2013) 2546–2550.
785 doi:10.1002/rcm.6717.
- 786 [35] K.T. Rinne, M. Saurer, K. Streit, R.T.W. Siegwolf, Evaluation of a liquid
787 chromatography method for compound-specific $\delta^{13}\text{C}$ analysis of plant
788 carbohydrates in alkaline media, *Rapid Commun. Mass Spectrom.* 26 (2012)
789 2173–2185. doi:10.1002/rcm.6334.
- 790 [36] R.S. Sevcik, R.A. Mowery, C. Becker, C.K. Chambliss, Rapid analysis of
791 carbohydrates in aqueous extracts and hydrolysates of biomass using a carbonate-
792 modified anion-exchange column, *J. Chromatogr. A.* 1218 (2011) 1236–1243.
793 doi:<https://doi.org/10.1016/j.chroma.2011.01.002>.
- 794 [37] H. Bauer, M. Claeys, R. Vermeylen, E. Schueller, G. Weinke, A. Berger, H.
795 Puxbaum, Arabitol and mannitol as tracers for the quantification of airborne
796 fungal spores, *Atmos. Environ.* 42 (2008) 588–593.
797 doi:10.1016/j.atmosenv.2007.10.013.
- 798 [38] P.M. Medeiros, M.H. Conte, J.C. Weber, B.R.T. Simoneit, Sugars as source
799 indicators of biogenic organic carbon in aerosols collected above the Howland
800 Experimental Forest, Maine, *Atmos. Environ.* 40 (2006) 1694–1705.

- 801 doi:10.1016/j.atmosenv.2005.11.001.
- 802 [39] B.R.T. Simoneit, Biomass burning — a review of organic tracers for smoke from
803 incomplete combustion, *Appl. Geochemistry*. 17 (2002) 129–162.
804 doi:10.1016/S0883-2927(01)00061-0.
- 805 [40] T.I. Eglinton, L.I. Aluwihare, J.E. Bauer, Ellen R.M.Druffel, A.P. Mcnichol, Gas
806 Chromatographic Isolation of Individual Compounds from Complex Matrices for
807 Radiocarbon Dating, *Anal. Chem.* 68 (1996) 904–912. doi:10.1021/ac9508513.
- 808 [41] T.I. Eglinton, G. Eglinton, L. Dupont, E.R. Sholkovitz, D. Montluc, C.M. Reddy,
809 Composition, age, and provenance of organic matter in NW African dust over the
810 Atlantic Ocean, *Geochemistry Geophys. Geosystems*. 3 (2002) 1525–2027.
811 doi:10.1029/2001GC000269.
- 812 [42] A. Ingalls, A. Pearson, Ten Years of Compound-Specific Radiocarbon Analysis,
813 *Oceanography*. 18 (2005) 18–31. doi:10.5670/oceanog.2005.22.
- 814 [43] M. Makou, T. Eglinton, C. McIntyre, D. Montluçon, I. Antheaume, V. Grossi,
815 Plant Wax n-Alkane and n-Alkanoic Acid Signatures Overprinted by Microbial
816 Contributions and Old Carbon in Meromictic Lake Sediments, *Geophys. Res.*
817 *Lett.* 45 (2018) 1049–1057. doi:10.1002/2017GL076211.
- 818 [44] A.L. Bour, B.D. Walker, T.A.B. Broek, M.D. McCarthy, Radiocarbon Analysis
819 of Individual Amino Acids: Carbon Blank Quantification for a Small-Sample
820 High-Pressure Liquid Chromatography Purification Method, *Anal. Chem.* 88
821 (2016) 3521–3528. doi:10.1021/acs.analchem.5b03619.
- 822 [45] C. Panagiotopoulos, D.J. Repeta, C.G. Johnson, Characterization of methyl
823 sugars, 3-deoxysugars and methyl deoxysugars in marine high molecular weight

- 824 dissolved organic matter, *Org. Geochem.* 38 (2007) 884–896.
825 doi:10.1016/j.orggeochem.2007.02.005.
- 826 [46] P.M. Medeiros, B.R.T. Simoneit, Analysis of sugars in environmental samples by
827 gas chromatography-mass spectrometry, *J. Chromatogr. A.* 1141 (2007) 271–
828 278. doi:10.1016/j.chroma.2006.12.017.
- 829 [47] X. Cheng, L.A. Kaplan, Simultaneous analyses of neutral carbohydrates and
830 amino sugars in freshwaters with HPLC-PAD, *J. Chromatogr. Sci.* 41 (2003)
831 434–438. doi: 10.1093/chromsci/41.8.434.
- 832 [48] E. Bard, T. Tuna, Y. Fagault, L. Bonvalot, L. Wacker, S. Fahrni, H.A. Synal,
833 AixMICADAS, the accelerator mass spectrometer dedicated to ¹⁴C recently
834 installed in Aix-en-Provence, France, *Nucl. Instruments Methods Phys. Res.*
835 *Sect. B Beam Interact. with Mater. Atoms.* 361 (2015) 80–86.
836 doi:10.1016/j.nimb.2015.01.075.
- 837 [49] M. Bretagnon, A. Paulmier, V. Garçon, B. Dewitte, S. Illig, L. Coppola, F.
838 Campos, F. Velazco, C. Panagiotopoulos, A. Oschlies, J.M. Hernandez-ayon, H.
839 Maske, O. Vergara, I. Montes, P. Martinez, E. Carrasco, J. Grelet, Desprez-De-
840 Gesincourt, C. Maes, L. Scouarnec, Modulation of the vertical particles transfer
841 efficiency in the Oxygen Minimum Zone off Peru, *Biogeosciences.* 15 (2018) 1–
842 19. doi:10.5194/bg-15-1-2018.
- 843 [50] C. Panagiotopoulos, R. Sempéré, V. Jacq, B. Charrière, Composition and
844 distribution of dissolved carbohydrates in the Beaufort Sea Mackenzie margin
845 (Arctic Ocean), *Mar. Chem.* 166 (2014) 92–102.
846 doi:10.1016/j.marchem.2014.09.004.

- 847 [51] C. Cheng, C.-S. Chen, P.-H. Hsieh, On-line desalting and carbohydrate analysis
848 for immobilized enzyme hydrolysis of waste cellulosic biomass by column-
849 switching high-performance liquid chromatography, *J. Chromatogr. A.* 1217
850 (2010) 2104–2110. doi:10.1016/j.chroma.2010.01.084.
- 851 [52] E.S. Gordon, M.A. Goni, Sources and distribution of terrigenous organic matter
852 delivered by the Atchafalaya River to sediments in the northern Gulf of Mexico,
853 *Geochim. Cosmochim. Acta.* 67 (2003) 2359–2375. doi:10.1016/S0016-
854 7037(02)01412-6.
- 855 [53] T.B. Coplen, W.A. Brand, M. Gehre, M. Gröning, H.A.J. Meijer, B. Toman,
856 R.M. Verkouteren, After two decades a second anchor for the VPDB $\delta^{13}\text{C}$ scale,
857 *Rapid Commun. Mass Spectrom.* 20 (2006) 3165–3166. doi:10.1002/rcm.
- 858 [54] T. Tuna, Y. Fagault, L. Bonvalot, M. Capano, E. Bard, Development of small
859 CO_2 gas measurements with AixMICADAS, *Nucl. Instruments Methods Phys.*
860 *Res. Sect. B Beam Interact. with Mater. Atoms.* 437 (2018) 93–97.
861 doi:10.1016/J.NIMB.2018.09.012.
- 862 [55] Y. Fagault, T. Tuna, F. Rostek, E. Bard, Radiocarbon dating small carbonate
863 samples with the gas ion source of AixMICADAS, *Nucl. Instruments Methods*
864 *Phys. Res. Sect. B Beam Interact. with Mater. Atoms.* (2019).
865 doi:10.1016/J.NIMB.2018.11.018.
- 866 [56] M. Stuiver, H.A. Polach, Reporting of C-14 data - Discussion, *Radiocarbon.* 19
867 (1977) 355–363.
- 868 [57] P.J. Reimer, T.A. Brown, R.W. Reimer, Discussion: Reporting and calibration of
869 post-bomb C-14 data, *Radiocarbon.* 46 (2004) 1299–1304.

- 870 [58] S.J. Angyal, G.S. Bethell, R.J. Beveridge, The separation of sugars and of polyols
871 on cation-exchange resins in the calcium form, *Carbohydr. Res.* 73 (1979) 9–18.
- 872 [59] C. Panagiotopoulos, O. Wurl, Spectrophotometric and chromatographic analysis
873 of carbohydrates in marine samples, in: O. Wurl (Ed.), *Pract. Guidel. Anal.*
874 *Seawater*, 1st Editio, CRC Press, Boca Raton, 2009: p. 408.
- 875 [60] C. Nobre, M.J. Santos, A. Dominguez, D. Torres, O. Rocha, A.M. Peres, I.
876 Rocha, E.C. Ferreira, J.A. Teixeira, L.R. Rodrigues, Comparison of adsorption
877 equilibrium of fructose, glucose and sucrose on potassium gel-type and
878 macroporous sodium ion-exchange resins, *Anal. Chim. Acta.* 654 (2009) 71–76.
879 doi:10.1016/j.aca.2009.06.043.
- 880 [61] J.A. Vente, H. Bosch, A.B. De Haan, P.J.T. Bussmann, Comparison of sorption
881 isotherms of mono- and disaccharides relevant to oligosaccharide separations for
882 Na, K, and Ca loaded cation exchange resins, *Chem. Eng. Commun.* 192 (2005)
883 23–33. doi:10.1080/00986440590473254.
- 884 [62] E.R.M. Druffel, P.M. Williams, J.E. Bauer, J.R. Ertel, Cycling of dissolved and
885 particulate organic matter in the open ocean, *J. Geophys. Res. Ocean.* 97 (1992)
886 15639–15659. doi:10.1029/92JC01511.
- 887 [63] M.H. O’Leary, Carbon Isotopes in Photosynthesis: Fractionation techniques may
888 reveal new aspects of carbon dynamics in plants, *Bioscience.* 38 (1988) 328–336.
- 889 [64] X.C. Wang, E.R.M. Druffel, Radiocarbon and stable carbon isotope compositions
890 of organic compound classes in sediments from the NE Pacific and Southern
891 Oceans, *Mar. Chem.* 73 (2001) 65–81. doi:10.1016/S0304-4203(00)00090-6.
- 892 [65] X.-C. Wang, J. Callahan, R.F. Chen, Variability in radiocarbon ages of

- 893 biochemical compound classes of high molecular weight dissolved organic
894 matter in estuaries, *Estuar. Coast. Shelf Sci.* 68 (2006) 188–194.
895 doi:10.1016/J.ECSS.2006.01.018.
- 896 [66] L.I. Aluwihare, D.J. Repeta, R.F. Chen, A major biopolymeric component to
897 dissolved organic carbon in surface sea water, *Nature*. 387 (1997) 166–169.
898 doi:10.1038/387166a0.
- 899 [67] D.J. Repeta, T.M. Quan, L.I. Aluwihare, A. Accardi, Chemical characterization
900 of high molecular weight dissolved organic matter in fresh and marine waters,
901 *Geochim. Cosmochim. Acta.* 66 (2002) 955–962. doi:10.1016/S0016-
902 7037(01)00830-4.
- 903 [68] C.F. Fortenberry, M.J. Walker, Y. Zhang, D. Mitroo, W.H. Brune, B.J. Williams,
904 Bulk and Molecular-Level Characterization of Laboratory-Aged Biomass
905 Burning Organic Aerosol from Oak Leaf and Heartwood Fuels, *Atmos. Chem.*
906 *Phys. Discuss.* 60 (2017) 1–40. doi:10.5194/acp-2017-576.
- 907 [69] A. Bertrand, G. Stefenelli, C.N. Jen, S.M. Pieber, E.A. Bruns, B. Temime-
908 Roussel, J.G. Slowik, A.H. Goldstein, I. El Haddad, U. Baltensperger, A.S.H.
909 Prévôt, H. Wortham, N. Marchand, Evolution of the chemical fingerprint of
910 biomass burning organic aerosol during aging, *Atmos. Chem. Phys. Discuss.*
911 (2018) 1–33. doi:10.5194/acp-2017-1196.
- 912 [70] L. Bonvalot, T. Tuna, Y. Fagault, J.-L. Jaffrezo, V. Jacob, F. Chevrier, E. Bard,
913 Estimating contributions from biomass burning and fossil fuel combustion by
914 means of radiocarbon analysis of carbonaceous aerosols: application to the
915 Valley of Chamonix, *Atmos. Chem. Phys. Discuss.* (2016) 1–39.
916 doi:10.5194/acp-2016-351.

- 917 [71] Z. Niu, S. Wang, J. Chen, F. Zhang, X. Chen, C. He, L. Lin, L. Yin, L. Xu,
918 Source contributions to carbonaceous species in PM_{2.5} and their uncertainty
919 analysis at typical urban, peri-urban and background sites in southeast China.,
920 Environ. Pollut. 181 (2013) 107–114. doi:10.1016/j.envpol.2013.06.006.
- 921 [72] A. Andersson, R.J. Sheesley, M. Kruså, C. Johansson, Ö. Gustafsson, 14C-Based
922 source assessment of soot aerosols in Stockholm and the Swedish EMEP-
923 Aspvreten regional background site, Atmos. Environ. 45 (2011) 215–222.
924 doi:10.1016/j.atmosenv.2010.09.015.

925

926

927

928

929

930

931

932

933

934

935

936 **Appendix A**

937 **Supporting data and information for**

938

939 **Liquid Chromatographic isolation of individual carbohydrates from** 940 **environmental matrices for stable carbon analysis and radiocarbon dating**

941

942 **Amel Nouara¹, Christos Panagiotopoulos^{1*}, Jérôme Balesdent², Kalliopi Violaki¹,**
943 **Edouard Bard², Yoann Fagault², Daniel James Repeta³, Richard Sempéré¹**

944

945 ¹Aix Marseille Univ., Université de Toulon, CNRS, IRD, MIO UM 110, 13288,
946 Marseille, France

947 ²Aix Marseille Univ., CNRS, Collège de France, IRD, INRA, CEREGE UM34, 13545
948 Aix-en-Provence, France

949 ³Department of Marine Chemistry and Geochemistry, Woods Hole Oceanographic
950 Institution, Woods Hole, MA 02543, USA

951

952 *Corresponding author. Phone: +33 4 86 09 05 26;

953 E-mail : christos.panagiotopoulos@mio.osupytheas.fr

954

955

956

957

958

959

960 February 27th, 2019

961

962

963 **Table of Contents**

964 **S 1. Optimization of the HPLC-RI system 44**

965 **S. 2. Supplementary figures and table legends 46**

966 **Fig. S1. Comparison of chromatograms with and without online degasser 46**

967 Fig. S2: Example of a standard monosaccharide mixture (50 μM each) purification on
968 (a) Ca^{2+} column: F_1 (glucose)/ F_2 (galactose + mannose)/ F_3 (fructose + arabinose)/ F_4
969 (galactosan)/ F_5 (mannitol)/ F_6 (levoglucosan)/ F_7 (sorbitol + xylitol)/ F_8 (mannosan),
970 followed by purification on (b) Pb^{2+} column of F_1 and F_2 fractions: $\text{F}_1 + \text{F}_{2-1}$
971 (glucose)/ F_{2-2} (galactose)/ F_{2-3} (mannose) and (c) Ca^{2+} column of F_{2-1} fraction : F_{2-1-1}
972 (unknown)/ F_{2-1-2} (glucose). Colored boxes correspond to peak(s) collection. 46

973 **Fig. S3.** Extracted ion chromatograms corresponding to the analysis of underivatized
974 levoglucosan (a), glucose (b) and galactose (c). The black line corresponds to the
975 respective authentic standard ($\sim 5\text{ppm}$ final concentration) and red line to the sample. In
976 all spectra, the molecular ion was detected as a Na^+ and NH_4^+ additive. More details are
977 given in Table S3. 47

978 Table S1: Columns characteristics and analysis conditions used for the HPLC-RI
979 system. 48

980 **Table S2.** Monosaccharide purification yields after three sequential purifications
981 ($\text{Ca}^{2+} \rightarrow \text{Pb}^{2+} \rightarrow \text{Ca}^{2+}$) of a standard monosaccharide mixture (see text) at 50 μM ($n = 3$).

982 49

983 **Table S3.** Theoretical and measured masses (LC-Q-TOF-MS analysis) recorded as Na^+
984 and NH_4^+ additives for levoglucosan, glucose and galactose. 49

985 **References** 50

986

987

988

989

990 **S 1. Optimization of the HPLC-RI system**

991 During the optimization step, a systematic large negative peak was always observed in
992 the chromatograms at 18-20 min (Fig. S1). Previous studies indicated that this peak is
993 probably due to the presence of dissolved oxygen in the sample and can mask the eluted
994 compounds at this time window or cause an increase in the baseline noise [1]. The peak
995 intensity somehow decreased after sample degassing (with pure He) but was still
996 significant at low sample concentrations. We overcame this problem by installing a
997 degassing device (RFIC eluent degasser, Thermo Fisher) before the chromatographic
998 column. We found that this device increases neither the back-pressure of the system nor
999 the retention time of the carbohydrates. To shorten the analysis time of the
1000 carbohydrates, no guard columns were used in this study. However, as a precaution, an
1001 online polyether ether ketone (PEEK) filter equipped with a stainless-steel frit (pore size
1002 0.5 μm) was placed just before the online degasser. The filter frit was cleaned regularly
1003 by sonication in a methanol bath, followed by sonication in ultrapure water, once per
1004 month and between each sample purification.

1005 Moreover, to maximize the collection efficiency of carbohydrates, the tubing between
1006 the RI detector and the fraction collector was minimized. The delay time between the
1007 detector and the fraction collector was calculated using 1 mM of vitamin B₁₂ without an
1008 analytical column. Further adjustments of the working flow rates (0.3 mL min⁻¹ and 0.6
1009 mL min⁻¹ for Na⁺ and Ca²⁺/Pb²⁺ columns, respectively) were made with a glucose
1010 standard (50 μM). We found that the highest recovery (~80%) of the glucose was
1011 obtained with a delay time of 110 s for the Na⁺ column, and 60 s for the Ca²⁺ and Pb²⁺
1012 columns. These delay times were applied for all peak and fraction collections during the
1013 purification procedure either of standards or samples.

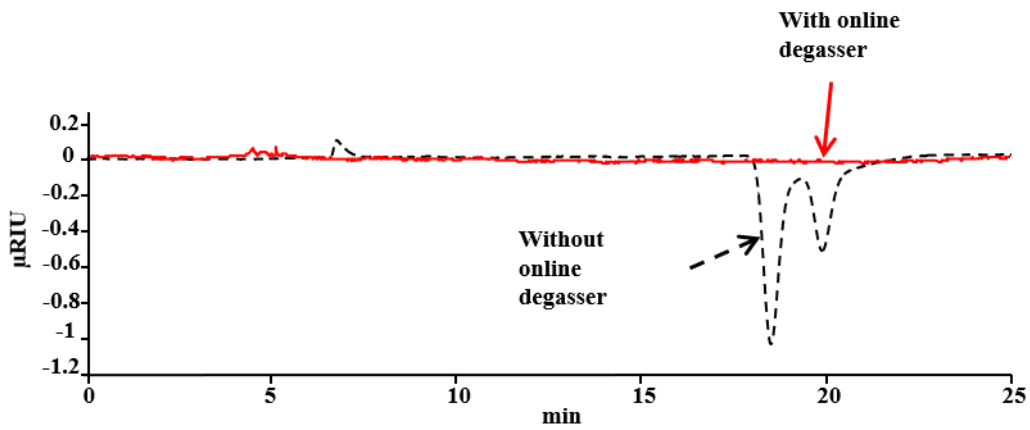
1014

1015

1016

1017 **S. 2. Supplementary figures and table legends**

1018

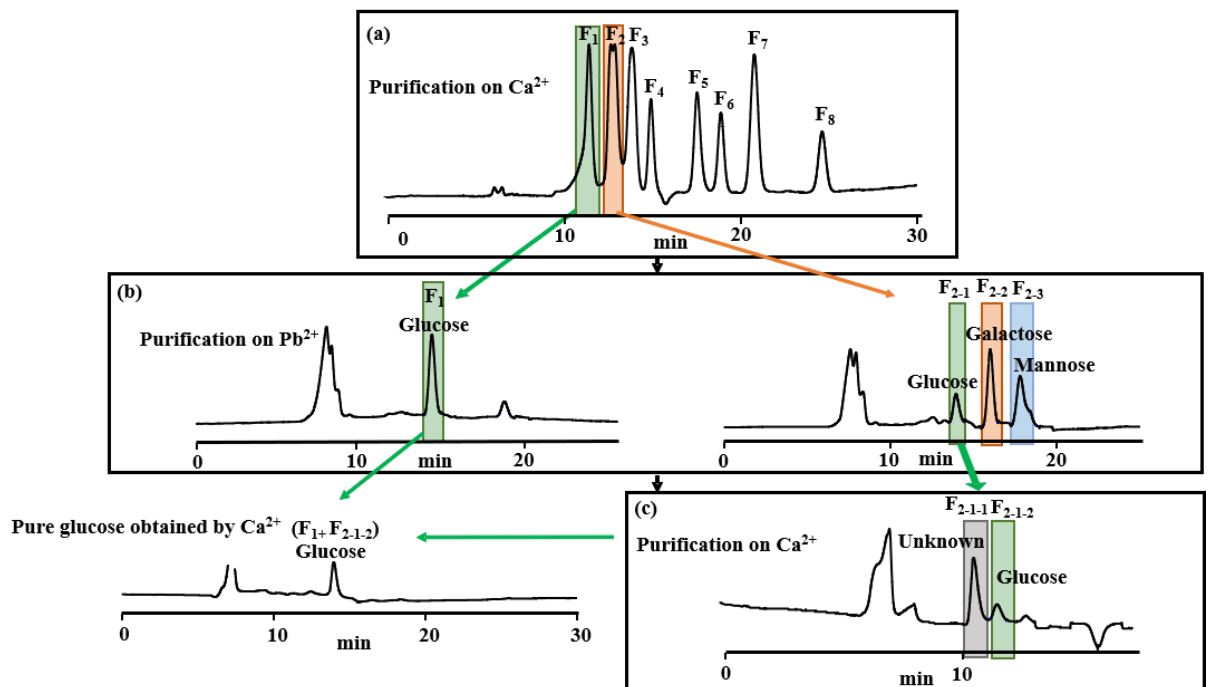


1019

1020 **Fig. S1.** Comparison of chromatograms with and without online degasser

1021

1022



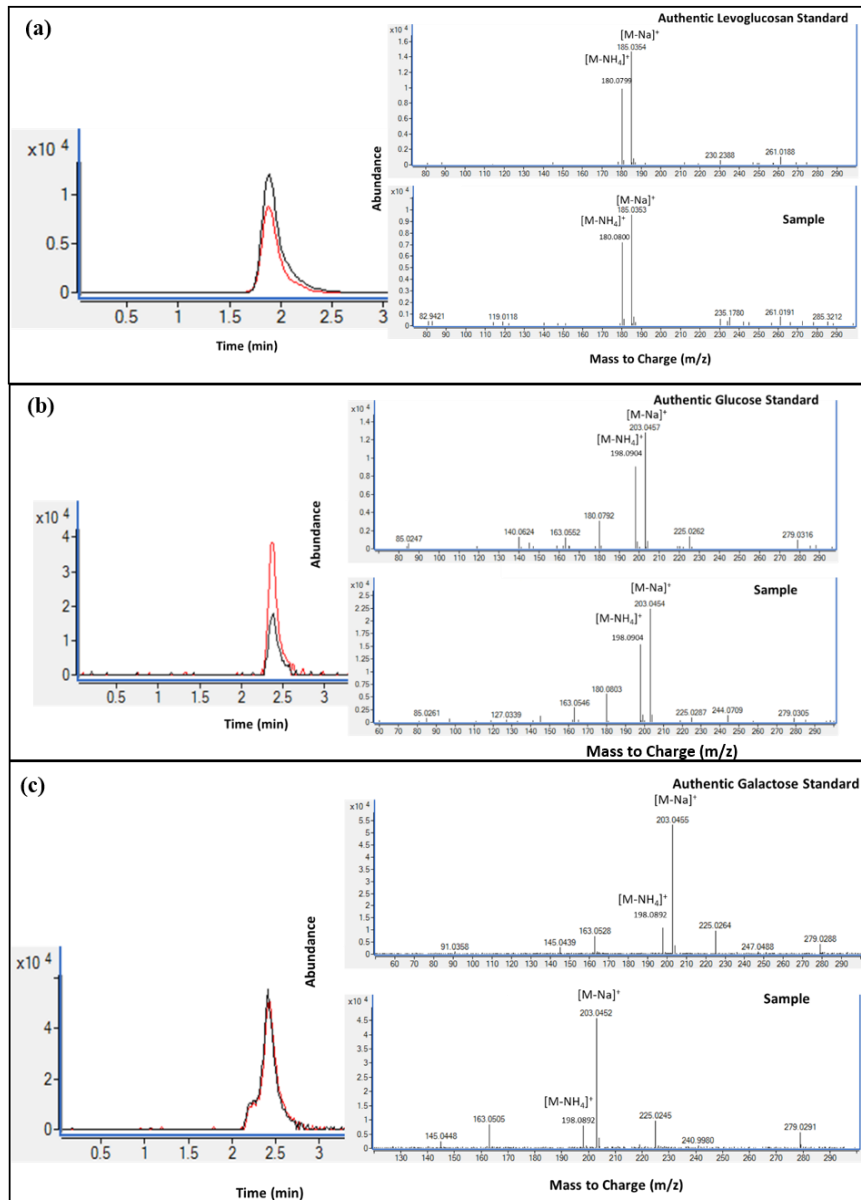
1023

1024 **Fig. S2:** Example of a standard monosaccharide mixture (50 μ M each) purification on

1025 (a) Ca^{2+} column: F₁ (glucose)/F₂ (galactose + mannose)/F₃ (fructose + arabinose)/F₄

1026 (galactosan)F₅ (mannitol)/F₆ (levoglucosan)/F₇ (sorbitol + xylitol)/F₈ (mannosan),

1027 followed by purification on (b) Pb^{2+} column of F_1 and F_2 fractions: $F_1 + F_{2-1}$
 1028 (glucose)/ F_{2-2} (galactose)/ F_{2-3} (mannose) and (c) Ca^{2+} column of F_{2-1} fraction : F_{2-1-1}
 1029 (unknown)/ F_{2-1-2} (glucose). Colored boxes correspond to peak(s) collection.
 1030



1031

1032

1033 **Fig. S3.** Extracted ion chromatograms corresponding to the analysis of underivatized
 1034 levoglucosan (a), glucose (b) and galactose (c). The black line corresponds to the
 1035 respective authentic standard (~ 5 ppm final concentration) and red line to the sample. In

1036 all spectra, the molecular ion was detected as a Na⁺ and NH₄⁺ additive. More details are
1037 given in Table S3.

1038

1039

1040

1041

1042 **Table S1:** Columns characteristics and analysis conditions used for the HPLC-RI
1043 system.

Column	RNO-Oligosaccharide	RCM-Monosaccharide	RPM-Monosaccharide
The ionic form	Na ⁺	Ca ²⁺	Pb ²⁺
Column size	200 × 10 mm	300 × 7.8 mm	300 × 7.8 mm
Stationary phase	Sulfonated styrene-divinylbenzene		
Cross linking	4%	8%	8%
Particles size	12 μm	9 μm	8 μm
Temperature	85 °C	85 °C	75 °C
Mobile phase	Degassed ultra-pure water		
Flow rate	0.3 mL min ⁻¹	0.6 mL min ⁻¹	0.6 mL min ⁻¹
Run time	50 min	30 min	45 min

1044

1045

1046 **Table S2.** Monosaccharide purification yields after three sequential purifications
 1047 ($\text{Ca}^{2+} \rightarrow \text{Pb}^{2+} \rightarrow \text{Ca}^{2+}$) of a standard monosaccharide mixture (see text) at 50 μM ($n = 3$).

Standard	Average yield
	Mean \pm Stdev
Glucose	36.32 \pm 0.02
Galactose	29.28 \pm 0.03
Mannose	25.17 \pm 0.01
Fructose	20.44 \pm 0.01
Arabinose	12.38 \pm 0.01
Galactosan	15.22 \pm 0.00
Mannitol	31.01 \pm 0.01
Levoglucosan	31.49 \pm 0.01
Xylitol	25.84 \pm 0.01
Sorbitol	30.09 \pm 0.03
Mannosan	32.21 \pm 0.00

1048

1049

1050

1051 **Table S3.** Theoretical and measured masses (LC-Q-TOF-MS analysis) recorded as Na^+
 1052 and NH_4^+ additives for levoglucosan, glucose and galactose.

Theoretical mass		Measured authentic standard mass		Measured purified compound mass	
Na^+	NH_4^+	Na^+	NH_4^+	Na^+	NH_4^+

	additive	additive	additive	additive	additive	additive
Levoglucosan (TSP)	185.0431	180.0877	185.0354	180.0799	185.0363	180.0800
Glucose (POM)	203.0537	198.0978	203.0457	198.0904	203.0454	198.0904
Galactose (POM)	203.0537	199.0978	203.0455	198.0892	203.0452	198.0892

1053

1054

1055 **References**

1056

1057 [1]X. Cheng, L. a Kaplan, Improved Analysis of Dissolved Carbohydrates in Stream

1058 Water with HPLC-PAD, Anal. Chem. 73 (2001) 458–461. doi:10.1021/ac001059r.

1059

1060